

WAVELET ANALYSIS FOR GEOPHYSICAL APPLICATIONS

Praveen Kumar
Hydrosystems Laboratory
Department of Civil Engineering
University of Illinois, Urbana

Efi Foufoula-Georgiou
St. Anthony Falls Laboratory
Department of Civil Engineering
University of Minnesota at Minneapolis-St. Paul

Abstract. Wavelet transforms originated in geophysics in the early 1980s for the analysis of seismic signals. Since then, significant mathematical advances in wavelet theory have enabled a suite of applications in diverse fields. In geophysics the power of wavelets for analysis of nonstationary processes that contain multiscale features, detection of singularities, analysis of transient phenomena, fractal and multifractal processes, and signal compression is now being exploited for the study of several processes including space-time precipitation, remotely

sensed hydrologic fluxes, atmospheric turbulence, canopy cover, land surface topography, seafloor bathymetry, and ocean wind waves. It is anticipated that in the near future, significant further advances in understanding and modeling geophysical processes will result from the use of wavelet analysis. In this paper we review the basic properties of wavelets that make them such an attractive and powerful tool for geophysical applications. We discuss continuous, discrete, orthogonal wavelets and wavelet packets and present applications to geophysical processes.

CONTENTS

Introduction	385
Time-frequency and time-scale analysis	387
Concept of frequency and scale	387
Time-frequency analysis	387
Wavelet transforms and time-scale analysis.....	389
Time-frequency localization using wavelets	391
Discrete and orthogonal wavelet transforms	392
Discrete wavelet transform	392
Orthogonal wavelet transform.....	393
Multiresolution analysis.....	396
Data analysis using wavelet transforms.....	397
Exploratory data analysis	397
Identification of scales of variation.....	397
Self-similar and fractal processes.....	400
Nonstationary processes	400
Numerical solution of partial differential equations	401
Wavelet packets and time-frequency-scale analysis	401
Two-dimensional applications.....	404
On the choice of wavelets.....	406
Summary and conclusions.....	408
Appendix: Computational aspects of orthogonal wavelet transforms.....	409

1. INTRODUCTION

Wavelet transforms are relatively recent developments that have fascinated the scientific, engineering,

and mathematics community with their versatile applicability. The following editorial quote from *Daubechies et al.* [1992, p. 529] gives us insight into the extent to which wavelets have become pervasive in various scientific and engineering research:

Wavelet transform has provided not only a wealth of new mathematical results, but also a common language and rallying call for researchers in a remarkably wide variety of fields: mathematicians working in harmonic analysis because of the special properties of wavelet bases; mathematical physicists because of the implications for time-frequency or phase-space analysis and relationships to concepts of renormalization; digital signal processors because of connections with multirate filtering, quadrature mirror filters, and subband coding; image processors because of applications in pyramidal image representation and compression; researchers in computer vision who have used "scale-space" for some time; researchers in stochastic processes interested in self-similar processes, $1/f$ noise, and fractals; speech processors interested in efficient representation, event extraction and mimicking the human auditory system. And the list goes on.

Within geophysics, there have been numerous applications already, such as in atmospheric turbulence for the detection of energy cascades and coherent structures; space-time rainfall for identification of scale-invariant symmetries; remotely sensed hydrometeorological and geological variables for data compression, noise reduction, and feature extraction; ocean wind waves for detection of wave breaking characteristics and phase relations during wind wave growth; and seafloor bathymetry for identification of the location of ridge-parallel faulting, among others (see *Foufoula-Georgiou and Kumar*

[1994] for a collection of papers on wavelet application in geophysics). The reason behind the versatility and attractiveness of wavelets for such diverse applications lies in their unique properties, and it is these properties that we seek to understand in this paper.

The wavelet transform originated in geophysics in the early 1980s for the analysis of seismic signals [Morlet *et al.*, 1982a, b] and was later formalized by Grössmann and Morlet [1984] and Goupillaud *et al.* [1984]. Wavelets found a nurturing atmosphere and the initial impetus in the signal processing and mathematics community, and within it, significant theoretical and application-oriented developments took place during the last 10 years or so. Important advances were made by Meyer [1992, and references therein], Mallat [1989a, b], Daubechies [1988, 1992], Chui [1992a], Wornell [1995], and Holschneider [1995], among others. These advances then impacted other areas of study and particularly applications in geophysics for process understanding. The developments and applications still continue at a very rapid pace.

Wavelets are essentially used in two ways when studying geophysical processes or signals: (1) as an integration kernel for analysis to extract information about the process and (2) as a basis for representation or characterization of the process. Evidently, in any analysis or representation the choice of the kernel or basis function determines the nature of information that can be extracted or represented about the process. This leads us to the following questions: (1) What kind of information can we extract using wavelets, and (2) how can we obtain a representation or description of a process using wavelets?

The answer to the first question lies in the important property of wavelets called time-frequency localization. The advantage of analyzing a signal, with wavelets as the analyzing kernels, is that it enables one to study features of the signal locally with a detail matched to their scale, i.e., broad features on a large scale and fine features on small scales. This property is especially useful for signals that are nonstationary, have short-lived transient components, have features at different scales, or have singularities. Therefore wavelets are apt to time-frequency and time-scale analysis.

The answer to the second question is based on seeing wavelets as elementary building blocks in a decomposition or series expansion akin to the familiar Fourier series. Thus a representation of the process using wavelets is provided by an infinite series expansion of dilated (or contracted) and translated versions of a mother wavelet, each multiplied by an appropriate coefficient.

The decision as to which representation (expansion) to use for a signal, for example, wavelet expansion versus Fourier or spline expansion, depends on the purpose of the analysis. Marr [1982, p. 21] remarks that

any particular representation makes certain information explicit at the expense of information that is pushed into the background and may be quite hard to recover. This issue is important, because how information is represented can greatly affect the ease with which one can do different things with it.

Therefore the purpose of the analysis is usually a guide to the selection of a particular representation. For a particular geophysical application one has to determine whether wavelet representation is needed in the first place and then to select the best wavelet representation for the problem at hand. This requires a good understanding of the properties of wavelets and how each property could be used for extracting certain information from a process.

For example, Fourier transforms provide a powerful tool for the analysis of stationary processes because for such processes the Fourier components are uncorrelated. Wavelet transforms provide us with a similar attractive property for a rich class of signals, namely, fractal or statistically self-similar signals. For instance, although fractional Brownian motion is a nonstationary and infinitely correlated process, its wavelet coefficients are stationary and practically uncorrelated.

One of the most important properties of wavelets, as remarked earlier, is time-frequency localization. This property is extensively discussed in section 2. We then describe the discrete and orthogonal wavelet transform in section 3. We discuss several example applications of wavelet transforms in section 4. Wavelet packets which offer a more flexible data-adaptive decomposition of a signal are discussed in section 5. Since several natural phenomena exhibit considerable spatial variability, two-dimensional wavelet transforms are important for the analysis of geophysical fields and are studied separately in section 6. Finally, we discuss some implementation issues related to the choice of wavelets and their impact on analysis and inference in section 7. We conclude with some recommendations for and speculations about further applications of wavelets for the study of geophysical processes.

There are several good introductory articles on different aspects of wavelets, for example, those by Mallat [1989a, b] and Rioul and Vetterli [1991], and the articles on turbulence, for example, by Fargé [1992a] and Fargé *et al.* [1996]. Also, considerable insight can be gained from the book reviews by Meyer [1993a] and Daubechies [1993]. Several works on wavelets have recently been published such as those by Meyer [1993b], Daubechies [1992], Benedetto and Frazier [1993], Chui [1992a, b], Ruskai *et al.* [1992], Fargé *et al.* [1993], Beylkin *et al.* [1991], and Meyer and Roques [1993]. Also, two special journal issues on wavelets (*IEEE Transactions on Signal Processing*, 41(12), 402 pp., 1993, and *Proceedings of the IEEE*, 84(4), 182 pp., 1996) include insightful expositions on the history and theory of wavelets and their applications to a variety of mathematical, engineering, biomedical, and turbulence problems, as well as future directions in wavelet research and applications. Fofoula-Georgiou and Kumar [1994] present a collection of papers which use wavelet transforms exclusively for the analysis of geophysical processes. An excellent nonmathematical overview on the various seed ideas in the development of wavelet transforms is given by Hubbard [1996].

2. TIME-FREQUENCY AND TIME-SCALE ANALYSIS

2.1. Concept of Frequency and Scale

The Fourier transform of a function $f(t)$ is given by [Papoulis, 1962]

$$\hat{f}(\omega) = \int_{-\infty}^{\infty} f(t)e^{-i\omega t} dt. \quad (1)$$

The original function can be recovered from the transform using

$$f(t) = \int_{-\infty}^{\infty} \hat{f}(\omega)e^{i\omega t} d\omega. \quad (2)$$

The parameter ω is the angular frequency of the periodic function $e^{-i\omega t}$, and therefore $\hat{f}(\omega)$ is said to represent the frequency content of the function $f(t)$. In the form of (2), $f(t)$ is understood to be represented as the “weighted sum” of the simple waveforms $e^{i\omega t}$, where the weight at a particular frequency ω is given by $\hat{f}(\omega)$.

Frequency is a physical attribute of a process or signal. For example, the propagation characteristics of a medium depend on the frequency of the traveling wave: Whereas light is unable to pass through aluminum, X rays can. Unlike frequency, which is a well-defined physical quantity and measured in cycles per second (or equivalent); different notions of scale exist depending upon the context. As explained by *Bloschl and Sivapalan [1995]*, in the context of geophysical applications, scale can be viewed from two perspectives, namely, “process scale” and “observation scale”. Process scale is the scale that natural phenomena exhibit and is beyond our control. Typically, this is characterized in terms of (1) the lifetime or duration, (2) the period, or (3) the correlation length of the process. On the other hand, the observation scale depends upon how we choose to measure the phenomena. Typically, this is characterized in terms of (1) the spatial or temporal extent or coverage, (2) the spacing between samples, or (3) the integration volume of a sample. In this paper, depending on the context, the term scale refers to either process scale, describing the lifetime or duration, or observation scale, describing the sampling interval.

For both continuous and discretely sampled processes the “resolution” refers to the smallest size of a feature that can be resolved, which means that resolution is related to the frequency content of a function or, more precisely, to the bandwidth of its spectrum [see *Rioul, 1993; Vetterli and Herley, 1992*]. If a continuous function $f(t)$ has a bandwidth ω_c (i.e., $\hat{f}(\omega) = 0$ for $|\omega| > \omega_c$), then the smallest size feature that exists is of wavelength $T = 2\pi/\omega_c$. If this function is sampled at a critical (Nyquist) rate, then all information about the continuous function is available in the discrete function. Sampling at a higher rate does not increase the resolution;

that is, an oversampled version of a function does not have more resolution than a critically sampled version. Note that a continuous function may have infinite resolution, as is the case with fractals, but for a discrete function its maximum resolution is determined by its sampling rate.

Scale and frequency (or wavelength) are independent attributes and are related to each other only through the fact that scale provides an upper bound to the wavelength, i.e., wavelength is less than or equal to scale. That is, a specific scale, for example, duration of a process, may contain frequencies from the smallest up to those dictated by the duration of the process.

2.2. Time-Frequency Analysis

Although the Fourier transform provides useful information about a signal, it is often not enough to characterize signals whose frequency content changes in time such as precipitation and many other geophysical processes. Figures 1a–1d illustrate the inapplicability of Fourier transforms for the characterization of time-varying signals. Although Fourier analysis tells us that there are two frequencies present in the signal, it is unable to distinguish between the two signals: one with two frequencies superimposed over its entire domain and the other with one frequency present in the first half of its domain and the other frequency present over the second half of its domain. To study such processes, we seek transforms that will enable us to obtain the frequency content of a process as a function of time. Such an analysis is called time-frequency analysis. The goal of time-frequency analysis is to expand a signal into waveforms whose time-frequency properties are adapted to the signal’s local structure. The waveforms that are used as building blocks in the expansion are called time-frequency atoms.

Wavelet transforms enable us to obtain orthonormal basis expansions of a signal using time-frequency atoms called wavelets that have good properties of localization in time and frequency domains. The basic idea can be understood using a time-frequency plane that indicates the frequency content of a signal at every time (see Figure 2). In any such decomposition the time-frequency plane is layered with cells, called Heisenberg cells, whose minimum area is determined by the uncertainty principle. Heisenberg’s uncertainty principle dictates that one cannot measure with arbitrarily high resolution in both time and frequency. When we use the standard basis in the time domain, that is, Dirac delta functions, we can very well localize the process in the time domain but not at all in the frequency domain. This is schematically depicted by tall thin boxes in Figure 2a. In the case of Fourier bases we get exact localization in frequency but none in time, which is depicted by long horizontal cells in Figure 2b. If we were to apply a moving window to the signal and to take the Fourier transform at every location in an attempt to localize the presence of a feature, we get a short time or windowed Fourier trans-

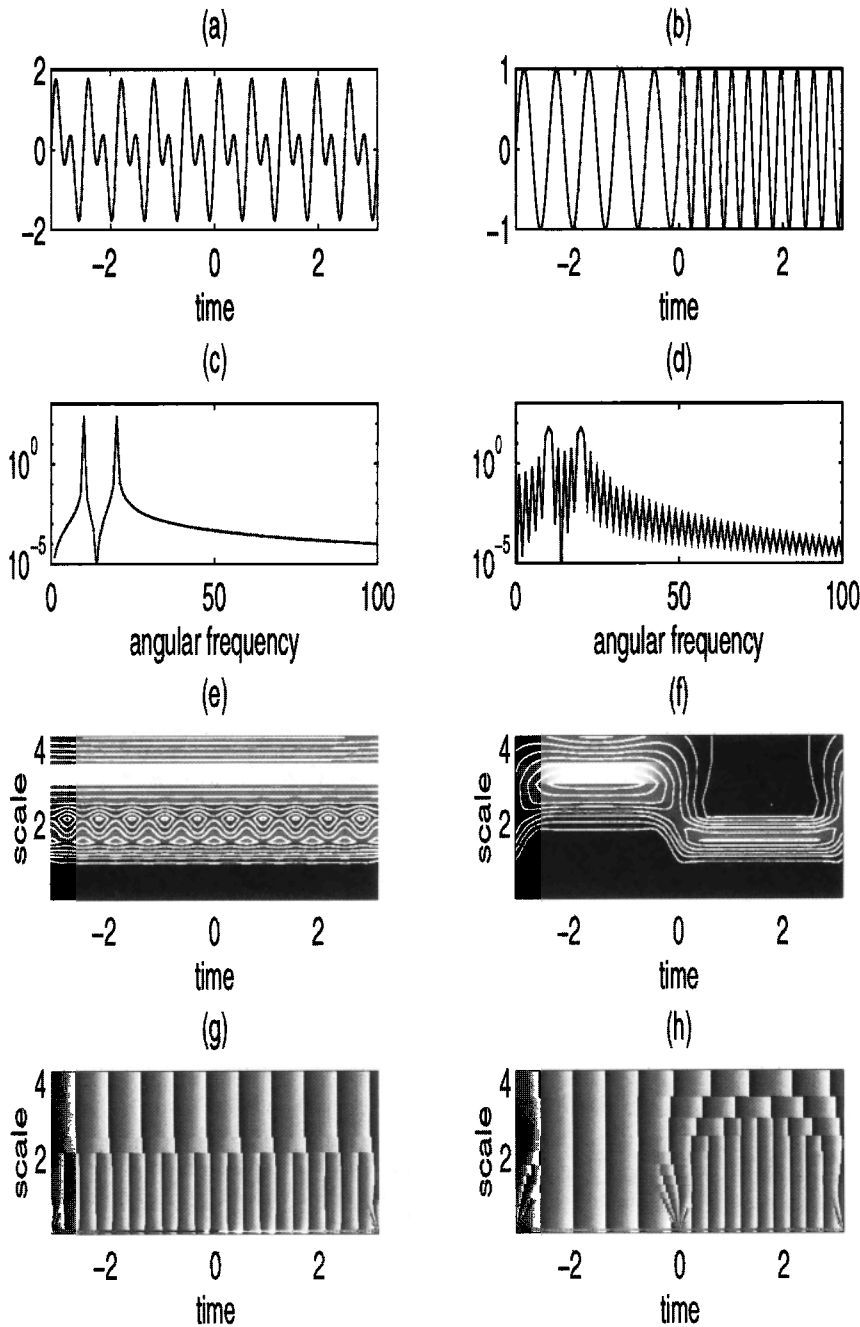


Figure 1. Spectral and wavelet analysis of two signals. The first signal (Figure 1a) consists of superposition of two frequencies ($\sin 10t$ and $\sin 20t$), and the second (Figure 1b) consists of the same two frequencies, each applied separately over half of the signal duration. Figures 1c and 1d show the Fourier spectra of the signals (i.e., $|f(\omega)|^2$ versus ω) for Figures 1a and 1b, respectively. Figures 1e and 1f show the magnitude of their wavelet transforms, and Figures 1g and 1h show the phase of their wavelet transforms (using Morlet wavelet). Notice the instability in calculation of phase at small scales where the modulus of wavelet transforms is very small.

form. This partitions the entire time-frequency plane with rectangular cells of the same size and aspect ratio (Figure 2c). The wavelet transform is based on an octave band decomposition of the time-frequency plane (Figure 2d). In this scheme, higher frequencies can be well localized in time, but the uncertainty in frequency localization increases as the frequency increases, which is reflected as taller, thinner cells with increase in frequency. Consequently, the frequency axis is partitioned finely only near low frequencies. The implication of this is that the larger-scale features get well resolved in the frequency domain, but there is a large uncertainty associated with their location. On the other hand, the small-scale features, such as sharp discontinuities, get well

resolved in the time (physical) domain, but there is a large uncertainty associated with their frequency content. This trade-off is an inherent limitation due to the Heisenberg's uncertainty principle (see section 2.4).

In all the above cases the decomposition pattern of the time-frequency plane, that is, layering of cells, is predetermined by the choice of the basis function. Note that the Heisenberg uncertainty principle dictates the minimum area of the cell and not its shape. So to further improve time-frequency analysis, we will want to layer the time-frequency plane using rectangular cells of arbitrary aspect ratios, with area greater than the minimum dictated by the uncertainty principle (see Figure 3). This can be achieved using wavelet packets by decoupling the

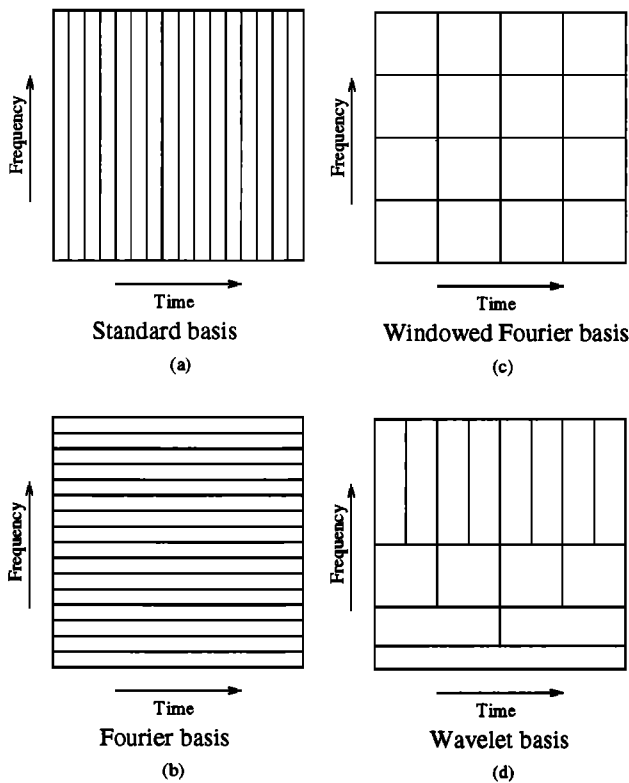


Figure 2. Schematic of time-frequency plane decomposition using different bases: (a) standard basis, (b) Fourier basis, (c) windowed Fourier basis, and (d) wavelet basis.

scale parameter from the frequency parameter (see section 5 for further discussions on wavelet packets).

2.3. Wavelet Transforms and Time-Scale Analysis

The wavelet transform of a function $f(t)$ is defined as the integral transform

$$Wf(\lambda, t) = \int_{-\infty}^{\infty} f(u) \bar{\psi}_{\lambda,t}(u) du \quad \lambda > 0, \quad (3)$$

where

$$\psi_{\lambda,t}(u) \equiv \frac{1}{\sqrt{\lambda}} \psi\left(\frac{u-t}{\lambda}\right) \quad (4)$$

represents a family of functions called wavelets. Here λ is a scale parameter, t is a location parameter, and $\bar{\psi}_{\lambda,t}(u)$ is the complex conjugate of $\psi_{\lambda,t}(u)$. Changing the value of λ has the effect of dilating ($\lambda > 1$) or contracting ($\lambda < 1$) the function $\psi(t)$ (see Figure 4), and changing t has the effect of analyzing the function $f(t)$ around different points t . When the scale λ increases, the wavelet becomes more spread out and takes only long time behavior of $f(t)$ into account and vice versa. Therefore the wavelet transform provides a flexible time-scale window that narrows when focusing on small-scale features and widens on large-scale features, analogous to a zoom lens. It is important to note that $\psi_{\lambda,u}(t)$

has the same shape for all values of λ . One may also interpret the wavelet transform as a mathematical microscope, where the magnification is given by $1/\lambda$ and the optics are given by the choice of wavelet $\psi(t)$.

The wavelet transform as defined by (3) is called the continuous wavelet transform (abbreviated CWT) because the scale and time parameters λ and t assume continuous values. It provides a redundant representation of a signal; that is, the CWT of a function at scale λ and location t can be obtained from the continuous wavelet transform of the same function at other scales and locations. The wavelet transform is a linear transform; that is, the wavelet transform of the sum of two signals is the sum of the wavelet transforms of each individual signal. Also, the wavelet transform of a vector function is a vector whose elements are the wavelet transforms of the vector components.

The inverse wavelet transform is given by [Daubechies, 1992, equation 2.4.4]

$$f(t) = \frac{1}{C_\psi} \int_{-\infty}^{\infty} \int_0^{\infty} \lambda^{-2} Wf(\lambda, u) \psi_{\lambda,u}(t) d\lambda du, \quad (5)$$

where C_ψ is constant, depending on the choice of the wavelet. Equation (5) can be looked at as a way of reconstructing $f(t)$ once its wavelet transform $Wf(\lambda, t)$ is known as well as a way to write $f(t)$ as a superposition of wavelets $\psi_{\lambda,t}(u)$.

The choice of the wavelet $\psi(t)$ is neither unique nor arbitrary. The function $\psi(t)$ is a function with unit energy (i.e., $\int |\psi(t)|^2 dt = 1$) chosen so that it has (1)

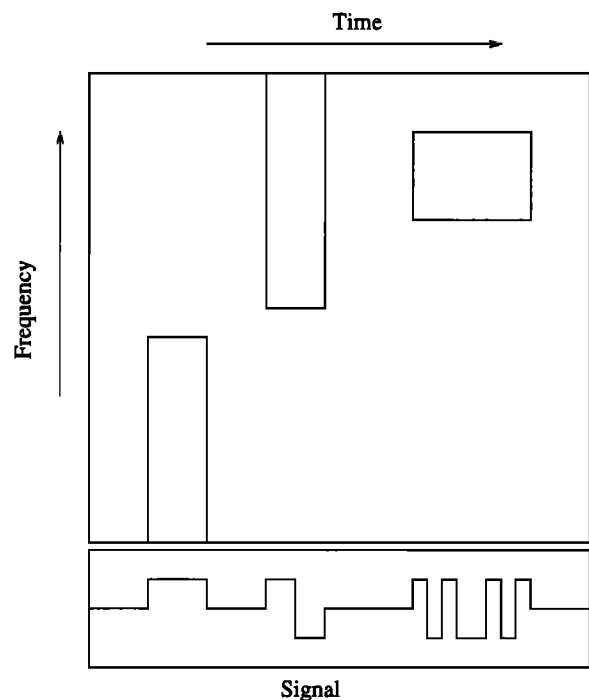


Figure 3. Schematic of time-frequency plane decomposition using wavelet packets.

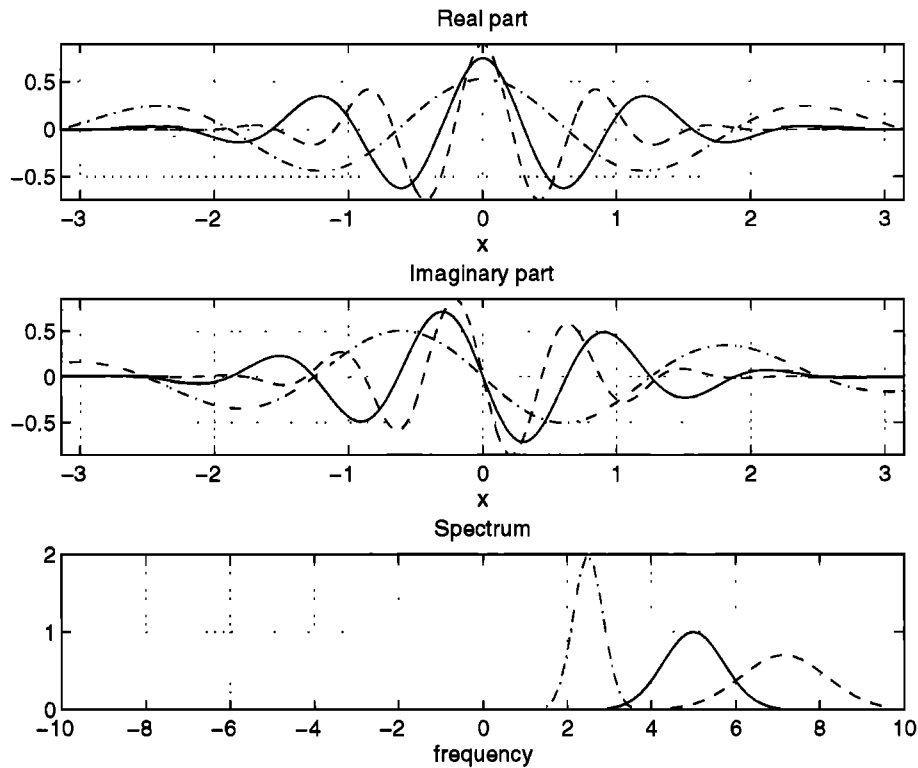


Figure 4. Real and imaginary parts of the Morlet wavelet ($\omega_0 = 5$) and its Fourier spectrum for different scales: $\lambda < 1$ (dashed lines), $\lambda = 1$ (solid lines), and $\lambda > 1$ (dash-dotted lines). Notice the effect of dilation on the wavelet and the corresponding change in its Fourier spectrum. When the wavelet dilates, its Fourier transform contracts, and vice versa. Also notice that the Fourier transform of the Morlet wavelet is supported entirely on the positive-frequency axis.

compact support, or sufficiently fast decay, to obtain localization in space and (2) zero mean (i.e., $\int_{-\infty}^{\infty} \psi(t) dt = 0$), although higher-order moments may also be zero, that is,

$$\int_{-\infty}^{\infty} t^k \psi(t) dt = 0 \quad k = 0, \dots, N - 1. \quad (6)$$

The requirement of zero mean is called the admissibility condition of the wavelet. It is because of the above two properties that the function $\psi(t)$ is called a wavelet. The second property ensures that $\psi(t)$ has a wiggle (i.e., is wave-like), and the first ensures that it is not a sustaining wave. The normalizing constant $1/\sqrt{\lambda}$ is chosen so that $\psi_{\lambda,t}(u)$ has the same energy for all scales λ .

As is evident, the two conditions described above leave open the possibility of using several different functions as wavelets. However, the choice is usually guided by various considerations and is discussed in some depth in section 7. Two popular wavelets for CWT are the Mexican hat and Morlet wavelet [see Daubechies, 1992]. The Mexican hat wavelet is the second derivative of the Gaussian function, given as

$$\psi(t) = \frac{2}{\sqrt{3}} \pi^{-1/4} (1 - t^2) e^{-t^2/2}. \quad (7)$$

The Morlet wavelet is given by

$$\psi(t) = \pi^{-1/4} e^{-i\omega_0 t} e^{-t^2/2} \quad \omega_0 \geq 5. \quad (8)$$

This wavelet is complex valued (see Figure 4), enabling one to extract information about the amplitude and phase of the process being analyzed (see Figures 1e–1h and Figure 5). Its Fourier transform, given by

$$\hat{\psi}(\omega) = \pi^{-1/4} \exp[-(\omega - \omega_0)^2/2] \quad \omega_0 \geq 5, \quad (9)$$

is approximately zero for $\omega < 0$. This is particularly attractive for certain analyses where one needs to eliminate the interference of positive and negative frequencies for the interpretation of results.

The wavelet transform is an energy-preserving transformation, that is

$$\int_{-\infty}^{\infty} |f(t)|^2 dt = \frac{1}{C_\psi} \int_{-\infty}^{\infty} \int_0^{\infty} |Wf(\lambda, t)|^2 \lambda^{-2} d\lambda dt. \quad (10)$$

In general, for two functions $f(t)$ and $g(t)$ [see Daubechies, 1992, equation 2.4.2],

$$\int_{-\infty}^{\infty} f(t) \bar{g}(t) dt = \frac{1}{C_\psi} \int_0^{\infty} \frac{1}{\lambda^2} \left(\int_{-\infty}^{\infty} Wf(\lambda, t) \overline{Wg(\lambda, t)} dt \right) d\lambda. \quad (11)$$

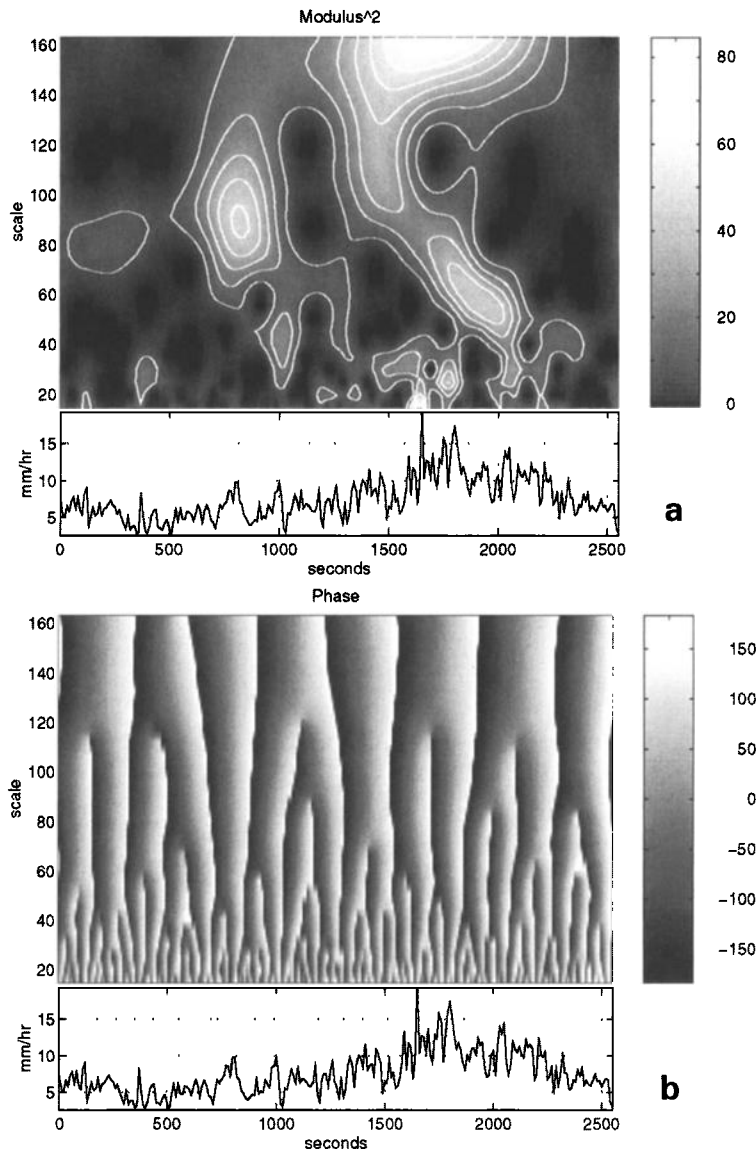


Figure 5. Analysis of temporal rainfall using the Morlet wavelet. The data were collected every 10 s on May 3, 1990, over Iowa City, Iowa, using an optical rain gage. (a) Square of the modulus or scalogram, that is, $|Wf(\lambda, t)|^2$, and (b) phase of $Wf(\lambda, t)$. The rainfall intensity is shown at the bottom of each figure. The scalogram clearly shows the presence of multiscale features and also some embedding of small-scale features within large-scale features. The phase plot shows the convergence of lines of constant phase to singularities (see discussion in text). (Reprinted by permission of Academic Press.)

Flandrin [1988] proposed calling the function $|Wf(\lambda, t)|^2$ a scalogram. In analogy, the product $Wf(\lambda, t)\overline{Wg(\lambda, t)}$ can be called a cross scalogram.

A scalogram provides an unfolding of the characteristics of a process in the scale-space plane. A cross scalogram provides the same unfolding of the interaction of two processes. This can be quite revealing about the structure of a particular process or about the interaction between processes. Figure 5a shows the scalogram of high-resolution temporal rainfall measured at a point every 10 s (for details on the data set and its measurement, see Georgakakos *et al.* [1994]). The presence of multiscale structures and their temporal locations are easily identified. Also, one can see embedding of some small-scale features within large-scale features. Figure 5b shows the phase plot of the wavelet transform. This figure illustrates that the constant-phase lines converge to a particular singularity as we go from large to small scales (although the computation of phase is unstable when the modulus of the wavelet transform is very

small). This enables us to identify the locations of singularities for further study, such as by fractal or multifractal analysis (for more extensive treatment of this idea, see Arnéodo *et al.* [1988]).

Liu [1994] defined a wavelet coherency function as

$$\Gamma = \frac{Wf(\lambda, t)\overline{Wg(\lambda, t)}}{|Wf(\lambda, t)||Wg(\lambda, t)|},$$

and using the Morlet wavelet, he studied the interaction between wind and ocean waves. He concluded that during wave growth the frequency components for peak wave energy between wind and waves are inherently in phase; that is, waves respond to wind speeds instantly. This result is in contrast to the belief that it is the “average” wind speed that is correlated to wave growth (see also Gambis [1992] for a similar application).

2.4. Time-Frequency Localization Using Wavelets

In order to understand the behavior of the wavelet transform in the frequency domain as well, it is useful to

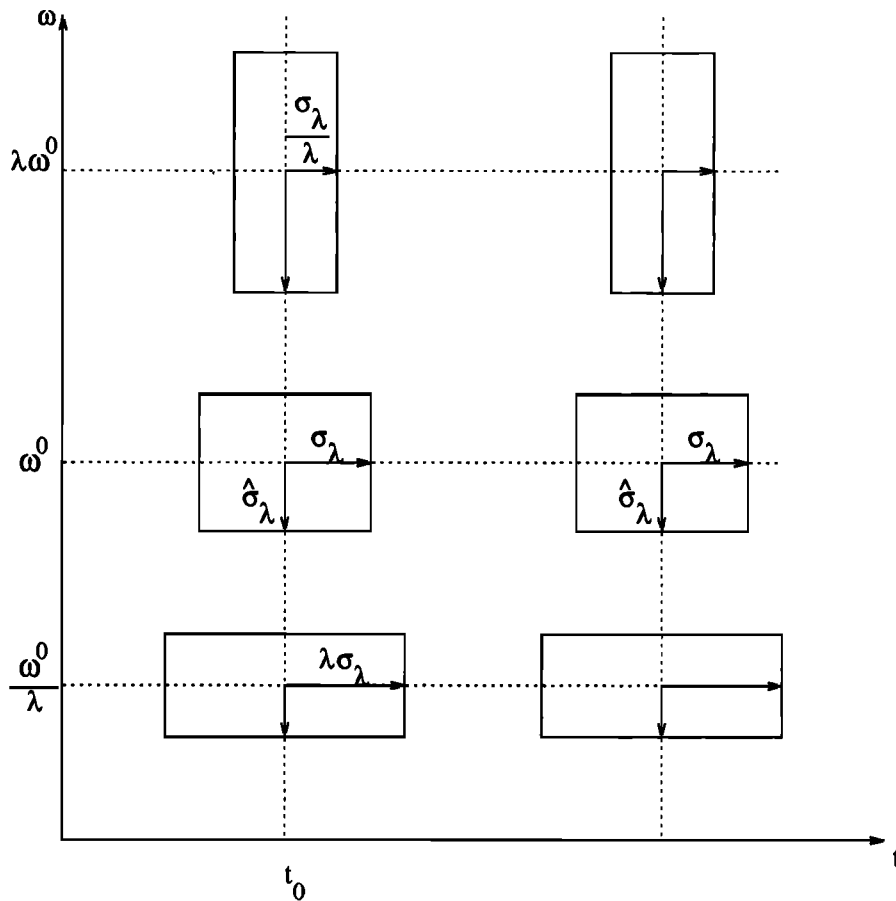


Figure 6. The phase-space representation using the wavelet transform.

recognize that the wavelet transform $Wf(\lambda, t)$, using Parseval's theorem, can be equivalently written as

$$Wf(\lambda, t) = \frac{1}{2\pi} \int_{-\infty}^{\infty} \hat{f}(\omega) \overline{\hat{\psi}_{\lambda,t}(\omega)} d\omega. \quad (12)$$

Therefore, to gain insight about the time-frequency localization properties of wavelet transforms, we consider the behavior of the following three parameters as a function of scale: (1) The standard deviation σ_λ of $|\psi_{\lambda,t}|^2$ satisfies $\sigma_\lambda = \lambda\sigma_1$. (2) The standard deviation $\hat{\sigma}_\lambda$ of $|\hat{\psi}_{\lambda,t}|^2$ satisfies $\hat{\sigma}_\lambda = \hat{\sigma}_1/\lambda$. (3) The center of passing band ω_λ^0 , which is defined as the mode of $|\hat{\psi}_{\lambda,t}|^2$ for either the positive or the negative frequency axis, satisfies $\omega_\lambda^0 = \omega_1^0/\lambda$.

From the above relationships one can easily see that as λ increases, that is, as the function dilates, both ω_λ^0 and $\hat{\sigma}_\lambda$ decrease, indicating that the center of the passing band shifts toward low-frequency components and the uncertainty also decreases, and vice versa (see also Figure 4). In the time-frequency plane (or phase space), the resolution cell for the wavelet transform around the point (t_0, ω_λ^0) is given by $[t_0 \pm \lambda\sigma_1 \times (\omega_1^0/\lambda) \pm (\hat{\sigma}_1/\lambda)]$, which has variable dimensions depending on the scale parameter λ (see Figure 6 and also Figure 2). However, the area of the resolution cell $[\sigma_\lambda \times \hat{\sigma}_\lambda]$ remains inde-

pendent of the scale or location parameter. In other words, the phase space is layered with resolution cells of varying dimensions which are functions of scale such that they have a constant area. Therefore, owing to the uncertainty principle, which states that both time and frequency cannot be measured with arbitrarily high precision, an increased resolution in the time domain for the time localization of high-frequency components comes at a cost: an increased uncertainty in the frequency localization as measured by $\hat{\sigma}_\lambda$. The localization properties of wavelets are discussed in further depth by Daubechies [1990] and Holschneider [1993].

3. DISCRETE AND ORTHOGONAL WAVELET TRANSFORMS

3.1. Discrete Wavelet Transform

In order to implement the wavelet transform on sampled signals we need to discretize the scale and location parameters. Wavelet transforms implemented on discrete values of scale and location are called discrete wavelet transforms. One can obtain both redundant and nonredundant representations using appropriate choices of wavelets and discretization schemes.

In discretizing the scale and location parameters (λ ,

t) one can choose $\lambda = \lambda_0^m$, where m is an integer and λ_0 is a fixed dilation step greater than 1. Since $\sigma_\lambda = \lambda\sigma_1$, we can choose $t = nt_0\lambda_0^m$, where $t_0 > 0$ depends upon $\psi(t)$ and n is an integer. The essential idea of this discretization can be understood by an analogy with a microscope. We choose a magnification (i.e., λ_0^{-m}) and study the process at a particular location and then move to another location. If the magnification is large (i.e., small scale), we move in small steps and vice versa. This is accomplished by choosing the incremental step inversely proportional to the magnification (i.e., proportional to the scale λ_0^m), which the above method of discretization of t accomplishes. We then define

$$\psi_{m,n}(t) = \frac{1}{\sqrt{\lambda_0^m}} \psi\left(\frac{t - nt_0\lambda_0^m}{\lambda_0^m}\right) = \lambda_0^{-m/2} \psi(\lambda_0^{-m}t - nt_0). \quad (13)$$

The wavelet transform obtained using $\psi_{m,n}(t)$ given as

$$Wf(m, n) = \lambda_0^{-m/2} \int f(t) \psi(\lambda_0^{-m}t - nt_0) dt \quad (14)$$

is called the discrete wavelet transform.

In the case of the continuous wavelet transform, $Wf(\lambda, t)$ completely characterizes the function $f(t)$. In fact, one could reconstruct $f(t)$ using (5). Using the discrete wavelet $\psi_{m,n}$ and appropriate choices of λ_0 and t_0 , we can also completely characterize $f(t)$. In fact, we can write $f(t)$ as a series expansion under certain broad conditions on the mother wavelet $\psi(t)$ and the discretization increments t_0 and λ_0 . These discrete wavelets which provide complete representation of the function $f(t)$ are called wavelet frames. The necessary and sufficient condition for this is that the wavelet coefficients $Wf(m, n)$ satisfy

$$A\|f\|^2 \leq \sum_m \sum_n |Wf(m, n)|^2 \leq B\|f\|^2.$$

Here $\|f\|^2$ denotes the energy (or \mathcal{L}^2 norm) of the function $f(t)$, and $A > 0$ and $B < \infty$ are constants characteristic of the wavelet and the choices of λ_0 and t_0 , which can be determined numerically [Daubechies, 1992]. Given this condition, we can obtain a series expansion as

$$f(t) = \frac{2}{A+B} \sum_m \sum_n Wf(m, n) \psi_{m,n} + \gamma \quad (15)$$

if $A \approx B$. The error term γ is of the order of $\varepsilon/(2 + \varepsilon)\|f\|$, where $\varepsilon = (B/A) - 1 \ll 1$.

In general, a frame is not an orthonormal basis (only the condition $A = B = 1$ gives an orthonormal basis). It provides a redundant representation of the function $f(t)$. This is analogous, for example, to representing a vector in the Euclidean plane using more than two basis vectors. The ratio A/B is called the redundancy ratio or redundancy factor. When a frame is redundant, the

wavelet coefficients in a neighborhood are correlated to each other, resulting in improved resolution of the sharp features of the signal being transformed. Thus, for example, for detecting a sharp change in a signal a redundant representation is useful. However, the oversampling also increases the computational complexity, resulting in slower transform and inverse transform algorithms.

Wavelets that provide a frame can be constructed for certain choices of λ_0 and t_0 . The conditions for the choice of λ_0 and t_0 are described by Daubechies [1992, chapter 3]. Here it suffices to say that these conditions are fairly broad and admit a very flexible range. For example, for the Mexican hat wavelet, for $\lambda_0 = 2$ and $t_0 = 1$, the frame bounds are $A = 3.223$ and $B = 3.596$, giving $B/A = 1.116$. One can obtain B/A closer to 1 by choosing $\lambda_0 < 2$. Grossmann *et al.* [1989] suggested decomposing each octave into several voices (as in music) by choosing $\lambda_0 = 2^{1/M}$, where M indicates the number of voices per octave. With this decomposition we get

$$\psi_{m,n}^M(t) = 2^{-m/2M} \psi(2^{-m/M}t - nt_0). \quad (16)$$

For the Mexican hat wavelet, by choosing $M = 4$ and $t_0 = 1$ we can obtain $A = 13.586$ and $B = 13.690$, giving $B/A = 1.007$. Such a decomposition using a multivoice frame enables us to cover the range of scales in smaller steps, giving a more “continuous” picture. For example, with $M = 4$ we get discrete scales at $\{\lambda = \dots, 1, 2^{1/4}, 2^{1/2}, 2^{3/4}, 2, 2^{5/4}, 2^{3/2}, 2^{7/4}, 4, \dots\}$ as against $\{\lambda = \dots, 1, 2, 4, \dots\}$ for the usual octave band decomposition, that is, $M = 1$. As an illustration, Figure 5 is obtained using the Morlet wavelet and four voices per octave. Multivoice frames are discussed extensively by Daubechies [1992, chapter 3], who gives more details on the values of A and B for different choices of M and t_0 for the Mexican hat and the Morlet wavelet. It should be noted that the discrete Morlet wavelet, which is not orthogonal, gives a good reconstruction under the framework of (15).

Redundant representations are more robust to noise as compared with orthogonal representations and therefore useful when noise reduction is an issue. Teti and Kritikos [1992] used only dominant coefficients from the entire set of $\{Wf(m, n)\}$, using the Morlet wavelet to obtain stable high-quality reconstruction of synthetic aperture radar (SAR) ocean image features (one-dimensional azimuth cross sections). With the reconstruction limited to dominant coefficients, filtering automatically takes place that gracefully reduces high-frequency information while still preserving image features. The filtering was successful in removing speckle while successfully preserving the scattering envelope of the ship and wake features.

3.2. Orthogonal Wavelet Transform

As was discussed in the Introduction and also in section 2, we often seek to decompose a function (or

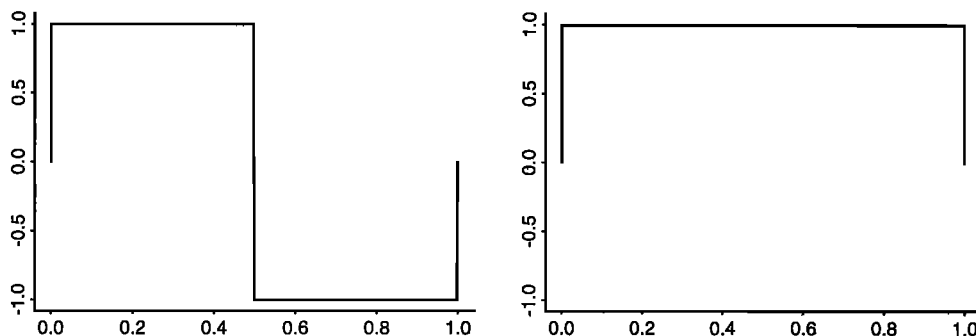


Figure 7. (left) The Haar wavelet and (right) the corresponding scaling function.

process) into components using basis functions (such as sines and cosines in the Fourier series expansions) in the hope that this decomposition will enable us to see something different about the process or enable us to perform certain operations on the process with greater ease. Usually, the choice of the basis set for decomposition is governed by the property that we wish to be revealed by the decomposition. The Fourier basis is a complete basis for the decomposition of the energy or variance. Another basis called the empirical orthogonal function (EOF) is also an appropriate basis for the decomposition of variance. In fact, EOFs are the most efficient bases for the decomposition of variance in that they capture the maximum variance with the least number of coefficients (or modes). However, both these basis sets (i.e., Fourier and EOFs) are “global” in the sense that they span the entire domain. Another disadvantage of EOFs is that they are “specific” in nature; that is, an optimal basis set for one data set will not necessarily be an optimal representation for another data set. In contrast, Fourier basis is a “universal” basis; that is, it can be used for efficient decomposition of any data set. Both the Fourier basis set and EOFs are orthogonal in that each “mode” of the decomposition carries information that is independent of the other modes.

For many signals that are nonstationary or whose frequency content changes over time, often the most desirable basis for decomposition of a signal is one that is orthogonal, local, and universal. Wavelet bases embody all these characteristics (see *Gamage and Blumen [1993]* for a comparative study of Fourier, EOF, and wavelet basis application in turbulence). We can find discrete wavelets $\psi_{m,n}(t)$ for $\lambda_0 = 2$ and $t_0 = 1$, that is,

$$\psi_{m,n}(t) = 2^{-m/2} \psi(2^{-m}t - n) = \frac{1}{\sqrt{2^m}} \psi\left(\frac{t - n2^m}{2^m}\right), \quad (17)$$

such that the set of functions $\{\psi_{m,n}\}$ for all m and n form an orthonormal basis. The most remarkable property of this basis is that the functions are orthogonal to their translates and their dilates [see *Mallat, 1989a*]. All square integrable functions $f(t)$ can be approximated, up to arbitrary high precision, by a linear combination of the wavelets $\psi_{m,n}(t)$, that is,

$$f(t) = \sum_{m=-\infty}^{\infty} \sum_{n=-\infty}^{\infty} D_{m,n} \psi_{m,n}(t), \quad (18)$$

where the first summation is over scales (from small to large) and at each scale we sum over all translates. From (18) it is easy to see how wavelets provide a time-scale representation of the process, where time location and scale are given by indices n and m , respectively. The coefficients $D_{m,n}$ are obtained as $D_{m,n} = \int f(t) \psi_{m,n}(t) dt$. Therefore the coefficient $D_{m,n}$ measures the contribution of scale 2^m at location $n2^m$ to the function. The total energy of the function can be obtained as $\int |f(t)|^2 dt = \sum_{m=-\infty}^{\infty} \sum_{n=-\infty}^{\infty} |D_{m,n}|^2$.

The above series expansion is akin to a Fourier series with the following differences: (1) The series is double indexed, with the indices indicating scale and location, and (2) the basis functions have the time-scale (time-frequency) localization property.

The Haar wavelet (see Figure 7) is the simplest of all orthogonal wavelets and is given as

$$\psi(t) = \begin{cases} 1 & 0 \leq t < \frac{1}{2} \\ -1 & \frac{1}{2} \leq t < 1 \\ 0 & \text{otherwise.} \end{cases} \quad (19)$$

For practical applications, often a smoother basis is desired. Bases with compact support and an arbitrary high order of smoothness have been developed, and a complete description is given by *Daubechies [1988, 1992]*, *Daubechies and Lagarias [1991, 1992]*, *Meyer [1992]*, and *Chui [1992a]*. An example of a wavelet developed by *Daubechies [1988]* called D8 is shown in Figure 8. It satisfies (6) for $N = 4$. As can be seen, it is a fairly smooth basis with very good localization properties in the Fourier domain.

Time-scale analysis, analogous to the continuous wavelet transform case, can be performed using orthogonal wavelets. For example, Figures 9a and 9c show the phase-space plot of the May 3, 1990, Iowa City, Iowa, temporal rainfall data (displayed in Figure 5) using the Haar (Figure 9a) and D8 (Figure 9c) wavelets. As is seen, most of the variability is concentrated in the large-

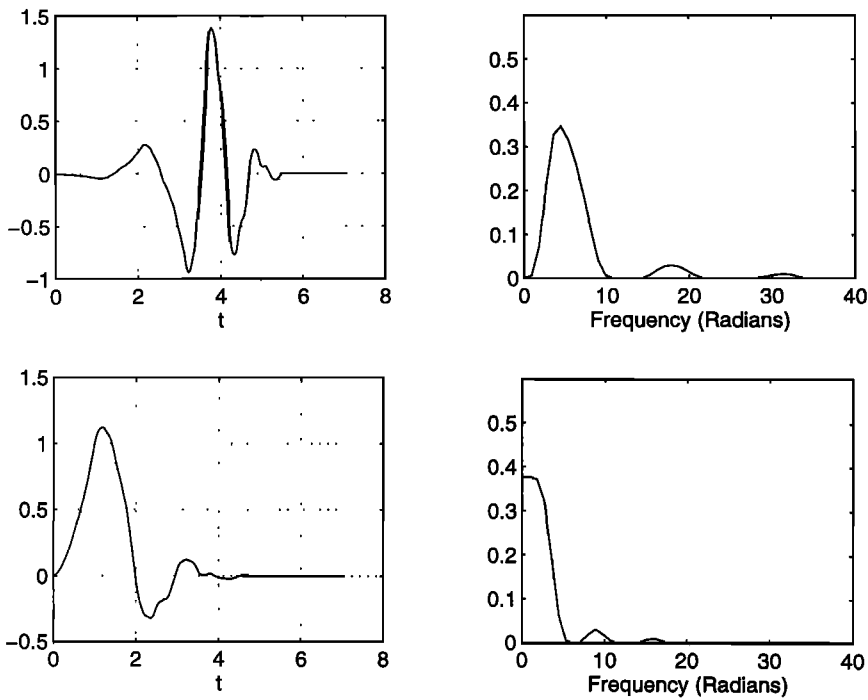


Figure 8. (top) Daubechies D8 wavelet [Daubechies, 1988] and its Fourier transform magnitude, and (bottom) the corresponding scaling function and its Fourier transform magnitude.

scale features, with small-scale features accounting for a relatively small fraction of the variability. Figures 9b and 9d show that relatively few wavelet coefficients can capture a significant portion of the variability (energy).

Also, it is noted that there is not a significant difference due to the choice of wavelets. Comparison of Figure 9 with Figure 5 shows that the phase-space plots using orthogonal wavelets and Morlet wavelet frames pick up

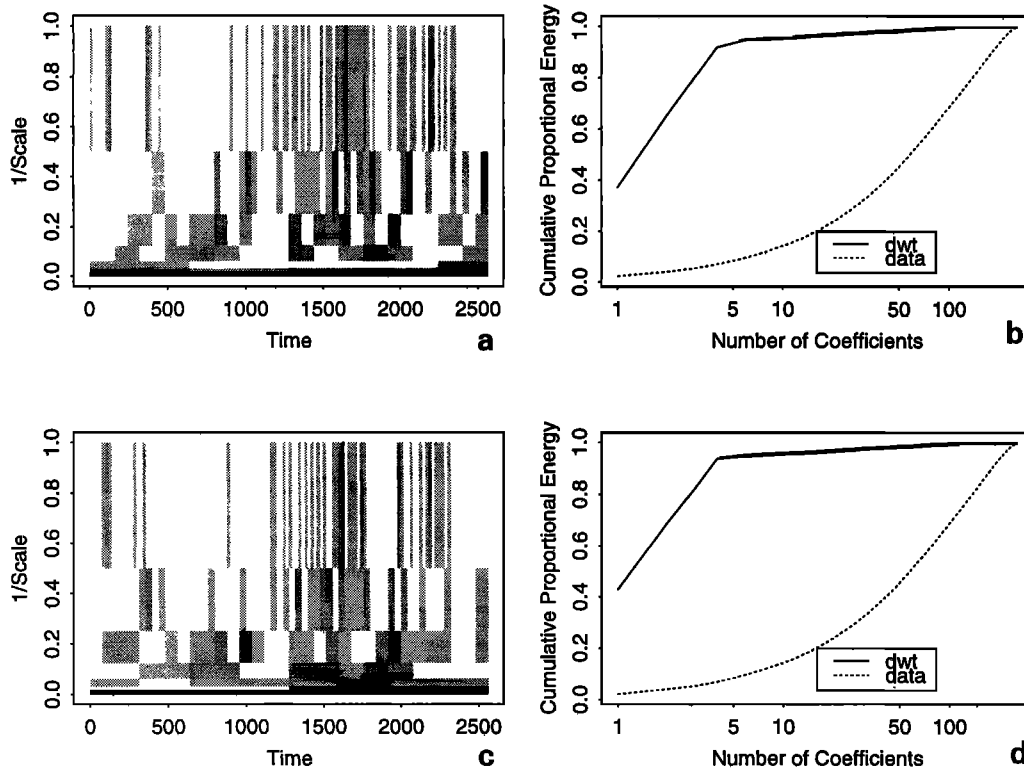


Figure 9. (left) Time-scale plot of the 10-s May 3, 1990, Iowa rainfall time series (see Figure 5) using (a) the orthogonal Haar wavelet and (c) the D8 wavelet. (b and d) The cumulative proportion of energy captured by the wavelet coefficients (solid line) and the data (dotted line) obtained by ordering the wavelet coefficients and data-sequence values from the largest to the smallest in absolute value.

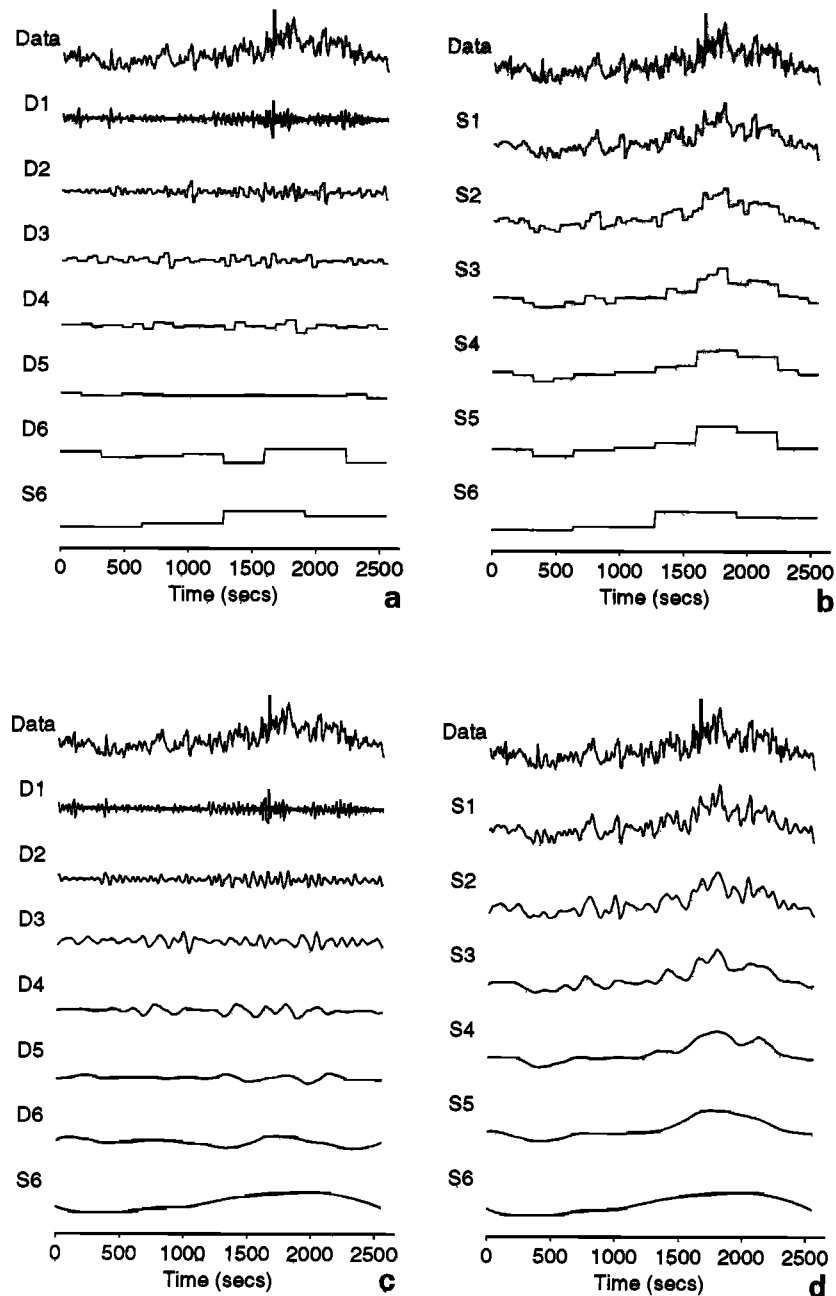


Figure 10. Illustration of multiresolution analysis. (b and d) The 10-s Iowa rainfall time series (see Figure 5) at decreasing resolutions, and (a and c) the detail that needs to be added to go from one resolution to the next. The general scheme of progression is $S_{\lambda-1} = S_{\lambda} + D_{\lambda}$. Analysis using (top) the Haar and (bottom) D8 wavelets.

similar information subject to the constraints of resolution of Heisenberg cells.

3.3. Multiresolution Analysis

One of the most profound applications of orthogonal wavelet transforms has been in multiresolution analysis. In some sense we can say that an entire class of orthogonal wavelets was developed [Daubechies, 1988] from the theory of wavelet-based multiresolution analysis of Mallat [1989a]. Multiresolution analysis is concerned with the study of signals or processes represented at different resolutions and developing an efficient mech-

anism for going from one resolution to another. To understand this, imagine that you are looking at a sequence of continuous functions such that the first function describes only broad features of a process (coarse resolution). Each subsequent function progressively adds more and more detail (higher resolution) such that smaller- and smaller-scale features start appearing as the resolution increases. For example, Figure 10b, represents the May 3, 1990, Iowa City rainfall data at decreasing resolutions (increasing scales $\lambda = 1, 2, \dots, 6$), and Figure 10a represents the corresponding wavelet transform obtained using the Haar wavelet. At the coarse

resolution level, all features larger than a particular scale are present. Let us represent this as $f_m(t)$ (i.e., function approximated by 2^{-m} samples per unit length in our notation so that as m decreases, i.e., scale decreases, the resolution increases). To get the function at the next higher resolution, we add some detail $f'_m(t)$, that is,

$$f_{m-1}(t) = f_m(t) + f'_m(t), \quad (20)$$

which is the basic recursive equation of multiresolution theory (in Figure 10 this is indicated as $S_{\lambda-1}(t) = S_\lambda(t) + D_\lambda(t)$, that is, $S_\lambda \equiv f_m(t)$, $S_{\lambda-1} \equiv f_{m-1}(t)$, and $D_\lambda \equiv f'_m(t)$). In the wavelet multiresolution framework, $f_m(t)$ is approximated as

$$f_m(t) = \sum_{n=-\infty}^{\infty} C_{m,n} \phi_{m,n}(t), \quad (21)$$

where $\phi_{m,n}(t) = 2^{-m/2} \phi(2^{-m}t - n)$ is a smoothing function. The coefficients $C_{m,n} = \int \phi_{m,n}(t) f(t) dt$ give the discrete sampled values of $f(t)$ at resolution m and location index n ; that is, the function $\phi(t)$, called the "scaling function," acts as a sampling function. The detail $f'_m(t)$ is approximated using orthogonal wavelets as

$$f'_m(t) = \sum_{n=-\infty}^{\infty} D_{m,n} \psi_{m,n}(t), \quad (22)$$

where the coefficients $D_{m,n}$ are defined as in (18). The scaling function $\phi(t)$ and wavelets $\psi(t)$ are related to each other, and one determines the other. For the Haar wavelet the scaling function is the characteristic function of the interval $[0, 1)$ (see Figure 7) given as

$$\phi(t) = \begin{cases} 1 & 0 \leq t < 1 \\ 0 & \text{otherwise.} \end{cases} \quad (23)$$

Figure 8 illustrates another example of a pair of scaling functions and wavelets. The scaling functions and wavelets play a profound role in the analysis of processes using orthogonal wavelets, as discussed in section 4.

4. DATA ANALYSIS USING WAVELET TRANSFORMS

4.1. Exploratory Data Analysis

Through exploratory data analysis (EDA) [Tukey, 1977], we aim to get a preliminary indication about the characteristics of the data and the nature of further analysis it calls for. Wavelet transforms offer a powerful tool for EDA where we can get an idea about the nonstationarity and the dominant scales of variation present in the series. As an example, consider Figure 11, which shows an exploratory data analysis of a $W'T'$ time series where W' and T' represent fluctuations in the vertical wind velocity and temperature, respectively. The data were obtained with a sampling frequency of 56 Hz over a dry lake bed in Owens Valley, California, on June 27, 1993 (see Katul et al. [1994] for a detailed description

of the data). The data were further subsampled by a factor of 2 to make the computation manageable. Figure 11a shows the time-frequency plot. The presence of intermittency in the sensible heat flux ($c_p W'T'$ where c_p is the specific heat capacity of air), characterized by sharp transitions which are manifested as high-frequency components, is clearly evident. Also evident is a slow increase in recurrence of these events. Figure 11b shows the distribution of energy at different scales. There seems to be some evidence of dominant scales of variations associated with scale indices $\lambda = 6$ and $\lambda = 8$, which correspond to timescales of 1.143 and 4.57 s, respectively. Figure 11c shows a summary of the distributions of wavelet coefficients at different scales using a box plot. The box indicates the interquartile range. The middle white strip indicates the median. The dynamic range is maximum for $\lambda = 8$, indicating significant activity at this scale. Figure 11d shows the energy concentration function (ecf), which for any sequence $\{a_n\}$ is defined as

$$\text{ecf}_a(k) = \frac{\sum_{n=0}^{k-1} a_{[n]}^2}{\sum_{n=0}^{N-1} a_n^2}, \quad (24)$$

where $a_{[n]}$ is the n th largest absolute value in $\{a_n\}$. Essentially, if $\text{ecf}_a(k) > \text{ecf}_b(k)$, then the first k -largest coefficients of the sequence $\{a_n\}$ contain more energy than those of $\{b_n\}$. The energy concentration function shows the disbalance in energy [Goel and Vidakovic, 1994] in the wavelet coefficients as compared with the data. This also indicates that relatively few wavelet coefficients describe the dominant characteristics of the data. This information can be used to characterize the dominant scales of variation in the data, as discussed next.

4.2. Identification of Scales of Variation

The need to identify significant structures from a passive or noisy component of a signal is an ubiquitous problem. In turbulence studies it arises often in the isolation of coherent structures. In signal processing, we are faced with the need to separate signal from noise. The wavelet spectrum defined as [see Meneveau, 1991a; Yamada and Ohkitani, 1991a; Hudgins et al., 1993a, b]

$$E(\lambda) = \int_{-\infty}^{\infty} Wf(\lambda, t) dt, \quad (25)$$

which for the orthogonal transform is given by

$$E(m) = \sum_n |D_{m,n}|^2 \quad (26)$$

has been quite useful for detecting the dominant scales or modes of variation. Notice that the wavelet spectrum condenses the scalogram (or phase plane) into a single function of scale. Gamage and Hagelberg [1993] explain that the wavelet spectrum can be compared with the Fourier spectrum (where the variance of the signal is decomposed as a function of wavelength). The main

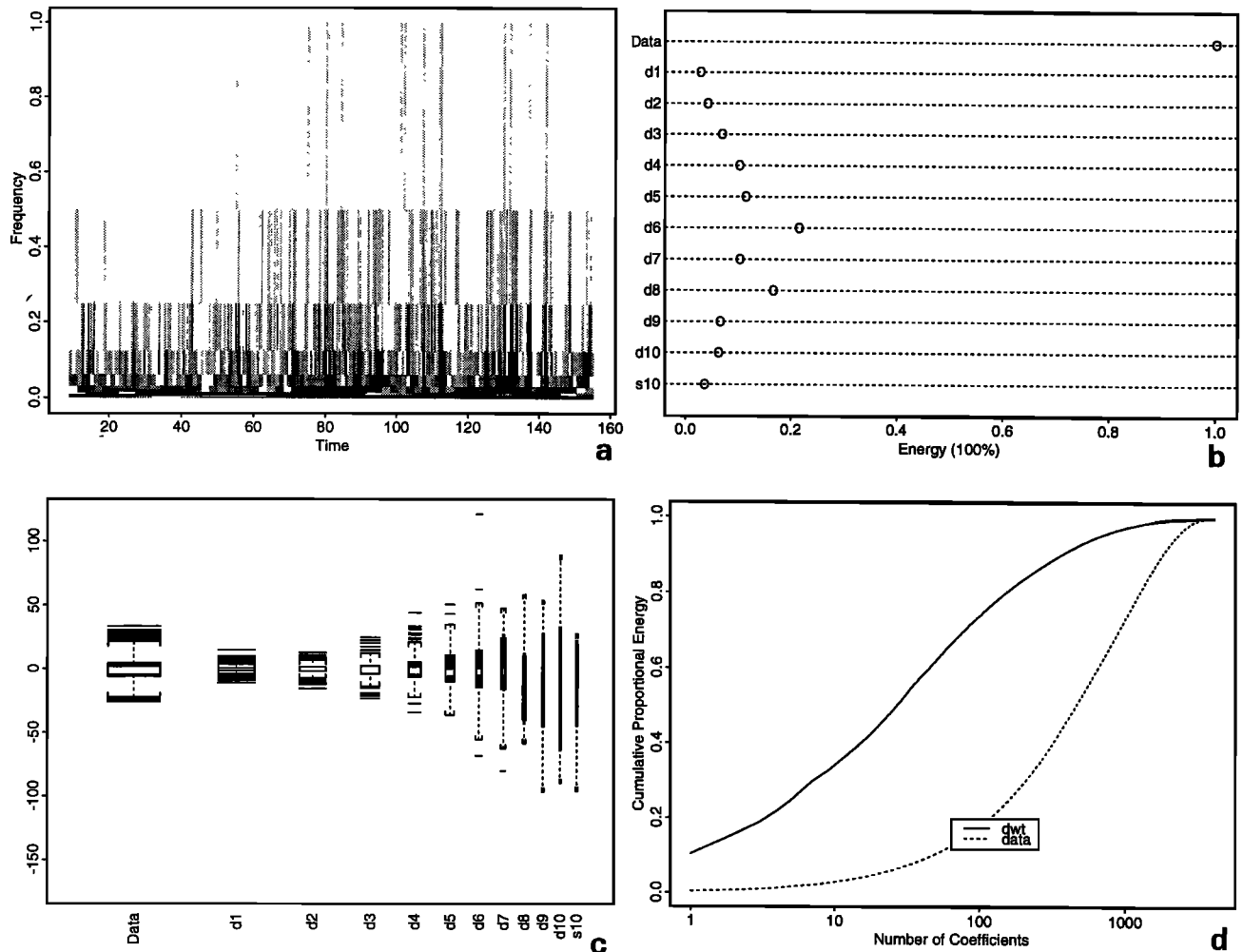


Figure 11. Exploratory data analysis of a $W'T'$ time series where W' and T' represent fluctuations in the vertical wind velocity and temperature, respectively. (a) Time-frequency plot. (b) Distribution of energy of wavelet coefficients at different scales λ identified through the labels $d\lambda$. The label $s\lambda$ indicates the information remaining in the data that is not captured by the wavelet coefficients. (c) Box plot of wavelet coefficients. The box indicates the interquartile range, and the middle white strip indicates the median. (d) Energy concentration function for the data and wavelet coefficients.

difference between the wavelet and Fourier decomposition is in the support of the respective basis functions. The wavelet transform coefficients are influenced by local events, while the Fourier coefficients are influenced by the function on its entire domain. This makes the wavelet spectrum a better measure of variance attributed to localized events.

Local maxima in the wavelet spectrum provide information about the scales at which important features or coherent events provide a significant contribution. This can happen in one of two ways: It can be due either to one feature with a large contribution or several small features with lesser contributions. Either or both situations might be present in a signal.

Variants of two techniques called “scale threshold partitioning” and “phase-plane threshold partitioning” [Hagelberg and Gamage, 1994] have been commonly employed to isolate the dominant modes of variation.

Scale threshold partitioning consists of reconstructing the signal using wavelet coefficients that contribute to the local maxima in the wavelet spectrum if there are clear scale gaps. Otherwise, one can just use all the wavelet coefficients for the scales that one perceives as dominant. In phase-plane partitioning, one performs reconstruction of the signal using wavelet coefficients whose amplitudes are above a certain threshold. In this case, a separation of signal and noise is achieved. This happens because in the case of wavelet transforms the presence of white noise in the signal gets smeared at all scales, thereby providing only small contributions at each scale, and is easily eliminated with an appropriate choice of threshold. There are various different rules for choosing a threshold, as discussed in detail by *Donoho and Johnston* [1994]. Often combination of scale and phase-plane thresholding provides an appropriate means for segregating signal characteristics.

Hagelberg and Gamage [1994] used the maxima of the wavelet variance as a means for identification of important scales in heat flux data measured using aircraft in the First International Satellite Land Surface Climatology Project (ISLSCP) Field Experiments (FIFE) [Sellers *et al.*, 1992]. They used scale threshold partitioning to separate the process into components with different dominant scales. Howell and Mahrt [1994] used wavelet-based mode separation techniques using the Haar wavelet to study turbulence data, each mode defined locally in terms of upper and lower cutoff scale. They partitioned the velocity field, measured 45 m above a flat terrain in near-neutral conditions, into four modes of variation and analyzed the coherent structure associated with each particular mode. Figure 12 shows these four modes of variation of a longitudinal wind component, which correspond to mesoscale ($c = 1$), large eddy ($c = 2$), transporting eddy ($c = 3$), and fine scale ($c = 4$).

Collineau and Brunet [1993a, b] showed that when a wavelet variance graph $E(\lambda)$ exhibits a single peak at a scale λ_0 , a characteristic duration scale D can be defined as

$$D = \lambda_0 D_\psi, \quad (27)$$

where D_ψ is a duration constant which is an intrinsic property of the wavelet $\psi(t)$. D_ψ can be computed as the solution of a simple first-order differential equation. Calculations for some common wavelets such as Mexican hat are given by Collineau and Brunet [1993a]. They demonstrated that D can be interpreted as the mean duration of the elementary events contributing most of the signal energy. For a sine function of period τ , $D = \tau/2$. Brunet and Collineau [1994] used these parameters to characterize the length scales of eddies above a maize crop, and after normalizing D with friction velocity (u_*) and canopy height (h), that is, using Du_*/h , they postulated that transfer processes over plant canopies are dominated by a population of canopy-scale eddies with universal characteristics. Gao and Li [1993], in a similar study over a deciduous forest, using a Mexican hat wavelet, observed that changes in wavelet variance with scales are characterized by local maxima. These local maxima can provide an objective method for determining the principal timescale of the coherent structures present in a signal. In time series of wind velocity these structures are observed as periodic patterns which are a manifestation of an ejection-sweep mechanism, corresponding to a slow upward movement of air followed by a strong downward motion associated with an acceleration of horizontal velocity. A similar technique was also used by Turner *et al.* [1994] in their study of turbulence over a forest canopy.

Meneveau [1991a, b] was the first to apply orthogonal wavelet transform expansion to the solution of Navier-Stokes equations. In comparing this approach with traditional Fourier-based approaches he argued that the wavelet approach allows more meaningful analysis of

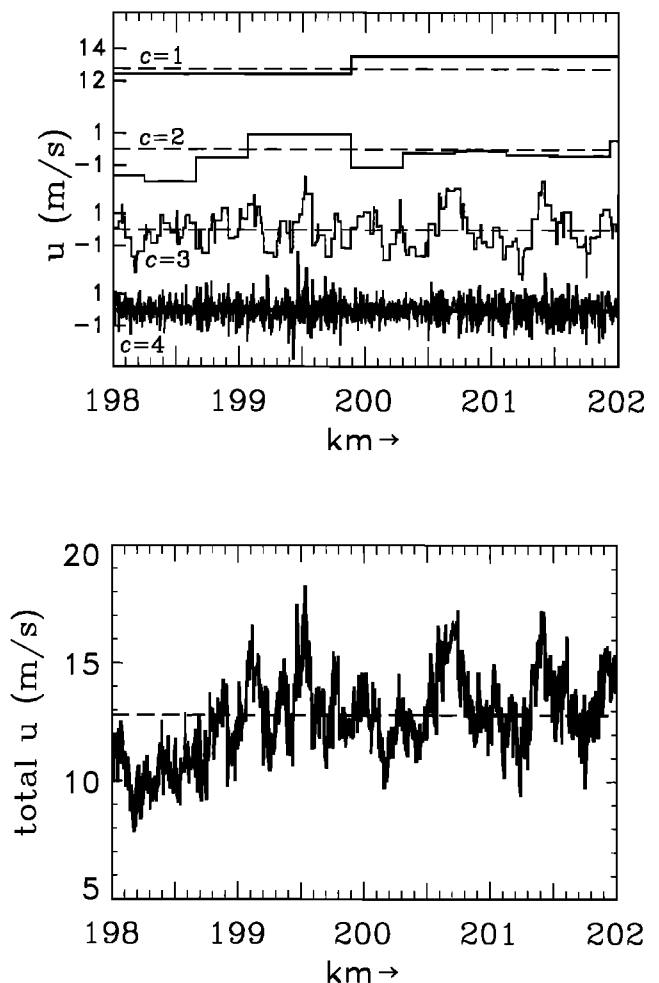


Figure 12. (top) The four orthogonal modes (mesoscale, $c = 1$; large eddy, $c = 2$; transporting eddy, $c = 3$; and fine scale, $c = 4$) of the longitudinal wind velocity component u measured 45 m above a flat terrain in near neutral conditions. (bottom) The sum of the four different modes which equals the original data. (Adapted from Howell and Mahrt [1994].) (Reprinted by permission of Academic Press.)

spatial properties at every scale, which is of great importance in the study of turbulence. He observed that the (orthogonal) wavelet-transformed Navier-Stokes equations were rather complicated but the appropriate contraction relevant to the energetics of turbulence was more transparent. He developed several statistical measures to study the spatial variability of the velocity field. Of significance is the concept of “dual spectra,” which gives information both about the contributions of various scales and about the spatial variability associated with each scale, which can be used to quantify the intermittency of the kinetic energy. He observed that the local kinetic energy can be described as a multifractal field. Similar studies in atmospheric turbulence have been performed by Yamada and Ohkitani [1990, 1991a, b], Hagelberg and Gamage [1994], Katul *et al.* [1994], Howell and Mahrt [1994], and Benzi and Vergassola [1991], among others.

4.3. Self-Similar and Fractal Processes

Orthogonal wavelet transforms are extremely useful for the analysis of self-similar (or simple scaling) processes, that is, processes that satisfy

$$\{X(\lambda t)\} \stackrel{d}{=} \{\lambda^H X(t)\} \quad \lambda > 0 \quad (28)$$

because of their ability to provide elegant multiscale transforms. Here $\stackrel{d}{=}$ indicates equality in (probability) distribution, and H is the scaling parameter. A typical example of a self-similar process is the fractional Brownian motion [Mandelbrot and Van Ness, 1968]. This process has a power law spectrum (i.e., $S(\omega) \approx 1/\omega^{2H+1}$). Mallat [1989b, equation (55)] has shown that for processes whose spectrum satisfies a power law the energy $E(m)$ of the detail signal (wavelet coefficients) satisfies the relationship

$$E(m) = 2^{2H}E(m + 1). \quad (29)$$

That is, the energies of the detail function at different resolutions (and hence at different scales) have a linear relationship on the logarithmic scale.

Wornell [1990] has described a method to construct self-similar processes from a set of uncorrelated random variables using orthonormal wavelet bases in the same spirit as Karhunen-Loève expansion. He showed that if we construct

$$X(t) = \sum_{m,n} d_{m,n} \psi_{mn}(t) \quad (30)$$

such that the sequences $\{d_{m,n}\}$ are uncorrelated for any distinct pairs m and m' and have a power law variance, that is, $\text{Var}(d_{m,n}) = (2^{-m})^{2H}E(m)$, then $X(t)$ is nearly self-similar, provided the wavelets satisfy a certain condition. The class of wavelets that satisfy this condition includes the Haar wavelet and the compactly supported wavelets constructed by Daubechies [1988]. The processes constructed this way retain the basic macroscopic spectral structure usually associated with self-similar processes. Construction of more complex self-similar processes, such as multifractal and multiaffine fields, based on wavelets has been presented by Benzi et al. [1993].

From the above results we see that wavelet transforms are very attractive for the study of self-similar processes. For instance, we obtain particularly simple expressions for the estimation of the scaling exponent H for a scaling process (see equation (29)) and an attractive recipe for the synthesis of second-order scaling processes (see equation (30)) using wavelets.

Flandrin [1988, 1992] has shown that for a fixed scale the wavelet transform of the fractional Brownian motion (FBM) is stationary. This result can be extended to conclude that the wavelet transform of any finite variance zero-mean process with self-similar stationary increments, at any fixed scale, when restricted to its second-order properties, behaves as a zero-mean covariance stationary process. Kumar and Fofoula-

Georgiou [1993a, Appendix B] further showed that the wavelet transform of a process with stationary increments of order N , using wavelets with N vanishing moments (see equation (6)), is a stationary process. Tewfik and Kim [1992] showed that although for a fixed scale the orthogonal wavelet coefficients of a FBM are stationary, these coefficients at different scales are correlated but the correlation function decays hyperbolically fast. This rate of decay increases with increase in the number of vanishing moments of the wavelets (see equation (6)) [see also Ramanathan and Zeitouni, 1991].

Percival and Guttorp [1994] argued that the usual variance is not an appropriate measure for studying long memory processes such as fractional Brownian motion. As an alternative they proposed using the Allan variance [Allan, 1966] because it can be estimated without bias and with good efficiency for such processes, and they showed that this variance can be interpreted as the Haar wavelet coefficient variance. They generalized this to other wavelets and illustrated their methodology with an application to time series of vertical ocean shear measurements.

4.4. Nonstationary Processes

One reason for the remarkable success of the Fourier transform in the study of stationary stochastic processes is the relationship between the autocorrelation function and the spectrum, as illustrated by the following diagram:

$$\begin{array}{ccc} X(t) & \begin{array}{c} \mathcal{F} \\ \rightleftharpoons \\ \mathcal{F} \end{array} & \hat{X}(\omega) \\ \downarrow & & \downarrow \\ R(\tau) = \mathcal{E}[X(t)X(t - \tau)] & \begin{array}{c} \mathcal{F} \\ \rightleftharpoons \\ \mathcal{F} \end{array} & S(\omega) = |\hat{X}(\omega)|^2 \end{array}$$

where $R(\tau)$ and $S(\omega)$ are the autocovariance function and the power spectrum of the stochastic process $X(t)$, respectively, \mathcal{E} indicates the expectation operator, and \mathcal{F} indicates the Fourier transform. If an analogous relationship could be developed for nonstationary processes using the wavelet transform, then the properties of the wavelet transform could be harnessed in a more useful way. It turns out that, indeed, such a relationship can be developed.

The wavelet variance $E(\lambda)$, although interesting in its own right, takes us away from the nonstationarity of the process since it is obtained by integrating over t . We therefore need something else. This is provided by the Wigner-Ville spectrum. Let us define a general (nonstationary) covariance function $R(t, s)$ as

$$R(t, s) = \mathcal{E}[X(t)X(s)].$$

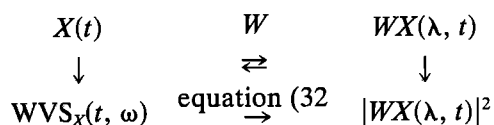
Then the Wigner-Ville spectrum (WVS) is defined as [see Claasen and Mecklenbrauker, 1980]

$$\text{WVS}_X(t, \omega) = \int_{-\infty}^{\infty} R\left(t + \frac{\tau}{2}, t - \frac{\tau}{2}\right) e^{-i\omega\tau} d\tau. \quad (31)$$

The $WVS_X(t, \omega)$ is an energy density function like the spectrogram. The relationship of interest to us is given by the relation between the scalogram and the WVS:

$$|WX(\lambda, t)|^2 = \int_{-\infty}^{\infty} \int_{-\infty}^{\infty} WVS_X(u, \omega) WVS_{\psi}\left(\frac{u-t}{\lambda}, \lambda\omega\right) du d\omega; \quad (32)$$

that is, the scalogram can be obtained by affine smoothing (i.e., smoothing at different scales in t and ω directions) of the WVS of X with the WVS of the wavelet. This relationship has been developed by *Flandrin* [1988]. As of this writing, we are unaware of any inverse relation to obtain the WVS_X from the scalogram. We can put the key result of this discussion in the following diagrammatic form:



This illustrates that there is an inherent link between the study of nonstationary processes and wavelet transforms akin to the link between stationary processes and Fourier transforms. Although we are not aware of any direct existing application of this property in geophysics, we anticipate that it will play a significant role in future studies since many geophysical processes are nonstationary.

4.5. Numerical Solution of Partial Differential Equations

Perrier [1990] argued that the spatial localization of wavelets allows precise approximation of discontinuities without producing spurious fluctuations all over the domain. Also, the asymptotic decrease of wavelet coefficients, at small scales, depends upon the local regularity of the analyzed function. Thus the largest coefficients will concentrate near discontinuities. He demonstrated the advantage of these properties by using orthogonal wavelet bases for the solution of the transport equation. *Qian and Weiss* [1993] compared a wavelet-Galerkin method with standard numerical methods for the numerical solution of the biharmonic Helmholtz equation and the reduced wave equation in nonseparable, two-dimensional geometry. They developed a method that is stable and spectrally accurate. They obtained accurate results for problems where, for instance, finite difference methods do not converge, or converge slowly, and where Fourier spectral methods do not apply. They used the wavelet multiresolution framework of *Mallat* [1989a] to formulate the problem and its solution scheme [see also *Glowinski et al.*, 1990; *Schultz and Wyld*, 1992; *Xu and Shann*, 1992].

5. WAVELET PACKETS AND TIME-FREQUENCY-SCALE ANALYSIS

We have seen that the conceptual key to understanding the success of the wavelet transform in addressing a wide range of problems is its property of time-frequency localization. However, the decomposition pattern of the time-frequency plane, that is, the layering of the cells, is predetermined by the choice of the basis function. Note that the Heisenberg uncertainty principle dictates the minimum area of the cell but not its shape. As was mentioned earlier, to further improve time-frequency analysis, we will want to layer the time-frequency plane with rectangular cells of arbitrary aspect ratios. These cells have an area greater than the minimum as dictated by Heisenberg's uncertainty principle, but the shape of the box, that is, the aspect ratio, is determined by the signal (or function) under study (see Figure 3).

Wavelet packets developed by *Coifman et al.* [1992a, b] accomplish this in an adaptive fashion by decoupling the scale and frequency parameter. They introduced a library of functions, called wavelet packets, from which a countably infinite number of orthogonal bases can be built. The infinitely many bases of wavelet packets consist of a set of localized oscillating functions $\psi_{\gamma}(t)$ of zero mean parameterized by position t , frequency ω , and scale λ . The index γ is defined as (t, ω, λ) . A wavelet packet family (a set of basis functions) is thus generated by translation, dilation, and modulation of a "mother wavelet" $\psi(t)$. The scale λ , position t , and frequency ω are the characteristic width of the spatial support, the position of the center, and the characteristic frequency of the basis function, respectively. It is noted here that wavelet packets can be constructed using any orthogonal wavelet (see *Wickerhauser* [1994] for details).

The entire collection of time-frequency atoms for all possible choices of the index set $\{(t, \omega, \lambda)\}$ provides a highly redundant set $D = \{\psi_{\gamma}(t)\}$ called a dictionary [Mallat and Zhang, 1993]. Figure 13 shows some basis elements generated using the Haar wavelet for different scale and frequency parameters. To efficiently represent any function $f(t)$, we must select an appropriate countable subset of atoms $\{\psi_{\gamma_n}(t)\}$ where $\gamma_n = (t_n, \omega_n, \lambda_n)$ so that $f(t)$ can be written as

$$f(t) = \sum_{n \in \Gamma} a_n \psi_{\gamma_n}(t), \quad (33)$$

where Γ is the subset of indices over which the series expansion is achieved. Depending upon the choice of the time-frequency atoms $\psi_{\gamma_n}(t)$, the coefficients a_n give explicit information on certain properties of $f(t)$. One needs to develop a procedure that chooses the atoms $\psi_{\gamma_n}(t)$ that are best adapted for decomposing the signal structures among all the time-frequency atoms of the large dictionary D . Compact expansions highlight the dominant features of $f(t)$ and allow $f(t)$ to be characterized by a few salient characteristics [Mallat and Zhang, 1993].

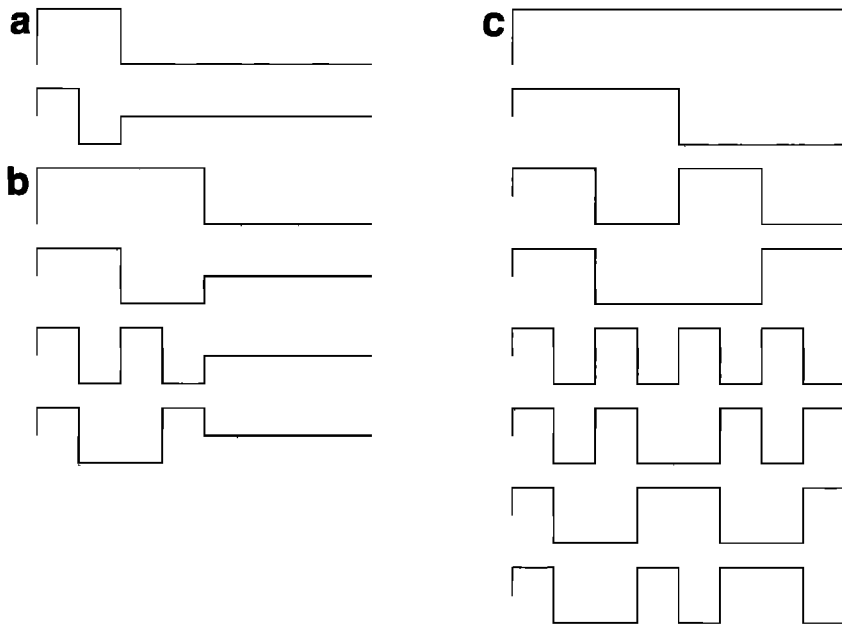


Figure 13. Wavelet packets generated from the Haar wavelet for three scales: (a) smallest scale, (b) intermediate scale, and (c) largest scale.

The objective then is to compute a linear expansion of $f(t)$ over a set of time-frequency-scale atoms selected from the dictionary $D = \{\psi_\gamma(t)\}$ in order to best match its inner structure. We discuss two algorithms, namely, entropy minimization and matching pursuits, to choose the coefficients that achieve the desired optimality in the representation (33). Both attempt to exploit the “disbalance” in the distribution of energy in the transformed domain, that is, fewer coefficients of the transform capturing significantly more energy than an equal number of data points when arranged in the order of decreasing energy [Goel and Vidakovic, 1994]. The more the energy is disbalanced, the better the performance of the algorithm.

The entropy minimization of the sequence $\{a_n\}$ is defined as

$$H(a) = -\sum_n p_n \log p_n, \quad p_n = \frac{|a_n|^2}{\sum_n |a_n|^2} \quad (34)$$

with $p_n \log p_n = 0$ if $p_n = 0$. The coefficients a_n , and consequently the basis functions $\psi_{\gamma_n}(t)$, are chosen so as to minimize $H(a)$. In entropy minimization, $\exp\{H(a)\}$ is proportional to the number of coefficients needed to represent the signal to a fixed mean square error. Thus minimizing entropy results in an orthonormal basis, termed “best basis,” which describes a function with the smallest possible number of coefficients with respect to the entropy cost function.

In the matching pursuit algorithm (developed by Mallat and Zhang [1993]), optimality is achieved through successive approximations of $f(t)$ with orthogonal projection on elements of the dictionary D . Let $\psi_{\gamma_0}(t) \in D$. The function $f(t)$ can be decomposed into

$$f(t) = \langle f, \psi_{\gamma_0} \rangle \psi_{\gamma_0}(t) + Rf(t), \quad (35)$$

where $Rf(t)$ is the residual vector after approximating $f(t)$ along $\psi_{\gamma_0}(t)$ and angle brackets represent an inner product. The functions $\psi_{\gamma_0}(t)$ are chosen such that the norm of the residual $\|Rf\|$ is minimum. This decomposition can be carried out recursively using $\psi_{\gamma_n} \in D$ to obtain

$$f(t) = \sum_{n=0}^p \langle R^n f, \psi_{\gamma_n} \rangle + R^{p+1}f(t). \quad (36)$$

The energy is partitioned as

$$\|f(t)\|^2 = \sum_{n=0}^p |\langle R^n f, \psi_{\gamma_n} \rangle|^2 + \|R^{p+1}f(t)\|^2. \quad (37)$$

The algorithm guarantees the convergence of the series as $p \rightarrow \infty$. The most important feature of this decomposition is that it is a greedy algorithm and in each recursion, optimization is carried out locally, in contrast to the global optimization in the entropy minimization.

A method using the matching pursuits algorithm to identify coherent structures was developed by Kumar [1996]. This method was able to reveal the essential dynamics of precipitation using the time-frequency-scale decompositions obtained from wavelet packets. It was argued that when the original function correlates well with a few dictionary elements, these correlated components represent “coherent structures” [Davis, 1994], and the remaining portion was called residue or noise with respect to the chosen dictionary. It is noted that although the term “coherent structure” as used here is not strictly in accordance with that used in the turbulence literature, it is not inconsistent with that notion. In turbulence the term is used to describe a region of flow over which at least one fundamental flow variable (ve-

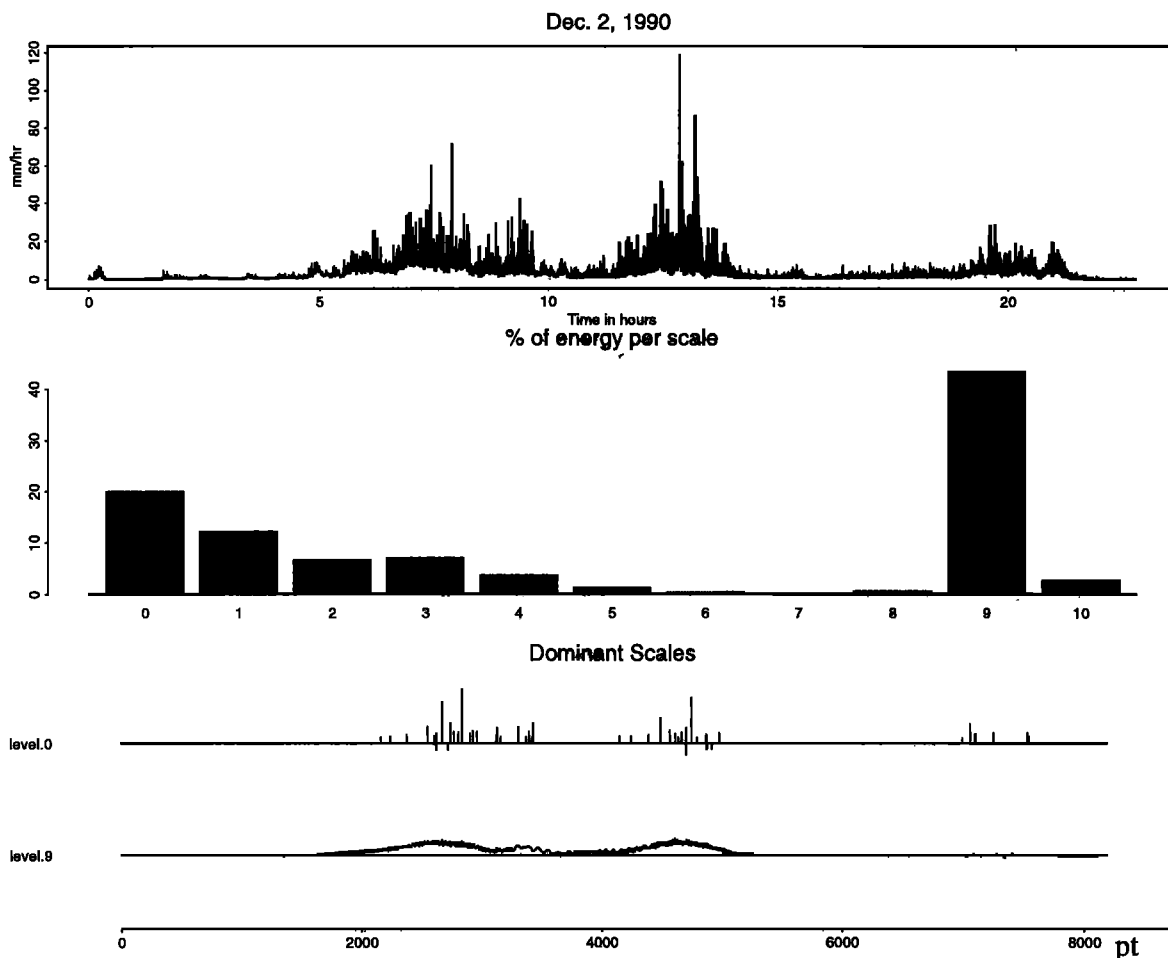


Figure 14. (top) Rainfall time series observed at a point in Iowa City on December 2, 1990. The data are available at 10-s sampling intervals and consist of 8192 points. (middle) Energy at different scales obtained using a wavelet packet decomposition with matching pursuits algorithm. Notice the two distinct scales of variation identified as convective and synoptic by Kumar [1996]. (bottom) Reconstruction of the fluctuations at the two dominant scales of variation.

locity, density, temperature, etc.) exhibits significant correlation with itself or with another variable [Robinson, 1991]. Here we use the term coherent structure to describe regions where the variable under study is significantly correlated with the basis elements, and these regions will have meaningful characteristics, provided the basis elements have meaningful properties. The choice of wavelet packets as basis elements enables us to identify fluctuations that persist or have a lifetime greater than their characteristic wavelength. We will also see that this does not exclude the possibility of identifying singularities as coherent structures, provided they have significant contribution to the variability of the process. The study applied the method to several temporal precipitation data sequences and was able to find the dominant scales of variation in the observed rainfall. Figure 14 illustrates the dominant scales of variation in a temporal rainfall sequence observed in Iowa City. Notice the large-scale high-frequency component and the reconstruction of the precipitation variability on

convective and synoptic scales using this method. This study showed that there exist distinct scales of variation, identifiable with rain cells and synoptic-scale activity, which is in contradistinction to the scale invariance hypothesis.

Venugopal and Foufoula-Georgiou [1996] used wavelet packets to study the energy distribution of rainfall over time, frequency, and scale in an effort to gain more insight into the rainfall-generating mechanism. Using high-resolution (5- and 10-s sampling interval) temporal rainfall series, they looked for the existence of persistent and short-lived structures and their associated frequencies and timescales, as well as the energy they carry. They then conjectured that the high-energy (high-frequency) short-lived structures may be associated with the convective portion of the rainfall event and that the low-energy (high- or low-frequency) persistent structures may be associated with the stratiform portion.

Fargé *et al.* [1992] applied wavelet packets for compressing two-dimensional turbulent flows. They defined their best basis as the one that minimized the enstrophy.

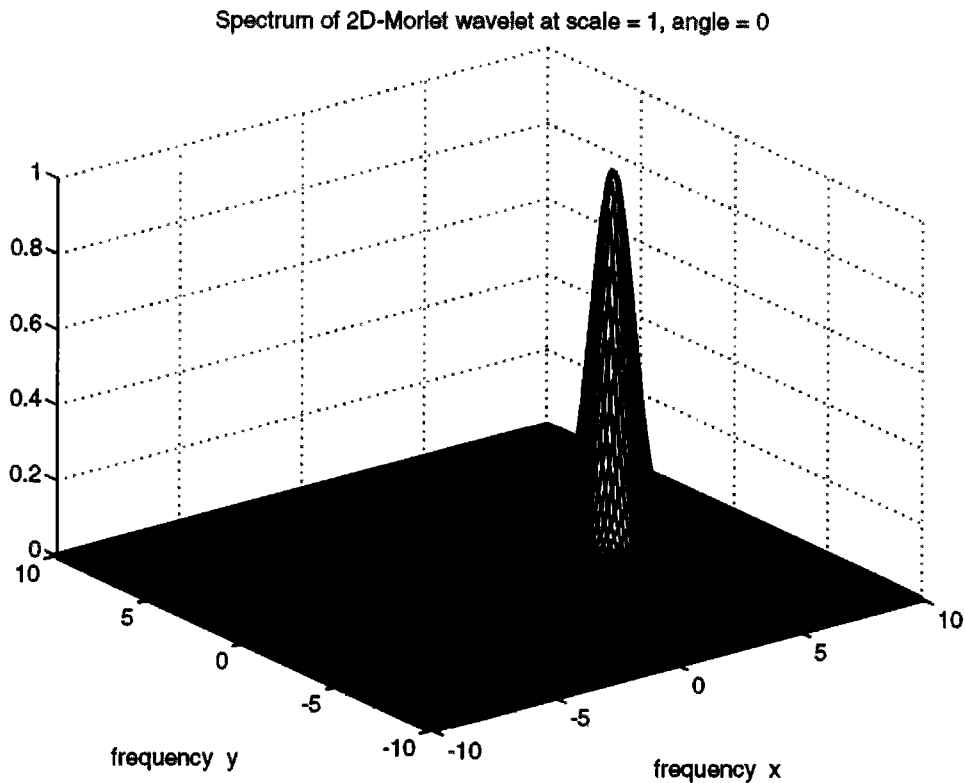


Figure 15. Frequency support of the two-dimensional Morlet wavelet [Kumar and Fofoula-Georgiou, 1994]. (Reprinted by permission from Academic Press.)

They found that the most significant wavelet packet coefficients in the best basis correspond to coherent structures and that the weak coefficients correspond to vorticity filaments. They were thus able to distinguish between a low-dimensional dynamically active part and a high-dimensional passive component.

Saito [1994] used wavelet packets for noise suppression and compression of geophysical signals containing transient features such as a migrated seismic section. The basic idea behind his scheme is that the signal component in the data may be represented by one or more of the bases in the library, whereas the noise component cannot be represented efficiently by any basis in the library [see also Wickerhauser, 1992].

6. TWO-DIMENSIONAL APPLICATIONS

The continuous two-dimensional wavelet transform is obtained by treating $\mathbf{u} = (u_1, u_2)$ and $\mathbf{t} = (t_1, t_2)$ as vectors in (3). Thus, for the two-dimensional case,

$$Wf(\lambda, \mathbf{t}) = \int_{-\infty}^{\infty} \int_{-\infty}^{\infty} f(\mathbf{u}) \psi_{\lambda, \mathbf{t}}(\mathbf{u}) d\mathbf{u} \quad \lambda > 0 \tag{38}$$

$$Wf(\lambda, \mathbf{t}) = \int_{-\infty}^{\infty} \int_{-\infty}^{\infty} f(\mathbf{u}) \frac{1}{\lambda} \psi\left(\frac{\mathbf{u} - \mathbf{t}}{\lambda}\right) d\mathbf{u}.$$

An analogous inversion formula also holds, that is,

$$f(\mathbf{t}) = \frac{1}{C_\psi} \int_{-\infty}^{\infty} \int_{-\infty}^{\infty} \int_{\lambda=0}^{\infty} \lambda^{-3} Wf(\lambda, \mathbf{u}) \psi_{\lambda, \mathbf{u}}(\mathbf{t}) d\lambda d\mathbf{u}. \tag{39}$$

The condition of admissibility of a two-dimensional wavelet remains the same, that is, (1) compact support or sufficiently fast decay and (2) $\iint \psi(\mathbf{t}) d\mathbf{t} = 0$.

As an example of the two-dimensional wavelet, we discuss the extension of the Morlet wavelet to two dimensions. Define the vector $\mathbf{t} = (t_1, t_2)$ on the two-dimensional plane with $|\mathbf{t}| = \sqrt{t_1^2 + t_2^2}$. Then the two-dimensional Morlet wavelet is defined as

$$\psi^\theta(\mathbf{t}) = \frac{1}{\sqrt{\pi}} \exp(-i\Omega^0 \cdot \mathbf{t}) \exp(-|\mathbf{t}|^2/2) \tag{40}$$

$$|\Omega^0| \geq 5$$

with Fourier transform (see Figure 15)

$$\hat{\psi}^\theta(\Omega) = \frac{1}{\sqrt{\pi}} e^{-|\Omega - \Omega^0|^2/2}, \tag{41}$$

where $\Omega = (\omega_1, \omega_2)$ is an arbitrary point on the two-dimensional frequency plane and $\Omega^0 = (\omega_1^0, \omega_2^0)$ is a constant. The superscript θ indicates the direction of the wavelet, that is,

$$\theta = \tan^{-1}(\omega_2^0/\omega_1^0). \tag{42}$$

The properties of this wavelet are best understood from its spectrum. Figure 15 shows the spectrum of the two-dimensional (2-D) Morlet wavelet for $\theta = 0$ and $\lambda = 1$. This wavelet is no longer progressive as in the one-dimensional case; that is, its spectrum is not entirely supported on the positive quadrant (although we still have a single lobe). Manipulating Ω^0 by changing θ allows us to change the directional selectivity of the wavelet. For example, by choosing $\Omega^0 = (\omega_1^0, \omega_2^0) = \omega^0(\cos \theta, \sin \theta)$, $\omega^0 \geq 5$, $0 \leq \theta \leq 2\pi$, we get the wavelet transform

$$W^\theta f(\lambda, \mathbf{t}) = \frac{\lambda}{\sqrt{\pi}} \int_{-\infty}^{\infty} \int_{-\infty}^{\infty} \hat{f}(\omega_1, \omega_2) \cdot \exp \left\{ -\lambda^2 \left[\left(\omega_1 - \frac{\omega_1^0}{\lambda} \right)^2 + \left(\omega_2 - \frac{\omega_2^0}{\lambda} \right)^2 \right] / 2 \right\} \cdot \exp [i(\omega_1 t_1 + \omega_2 t_2)] d\omega_1 d\omega_2. \quad (43)$$

That is, the wavelet transform $W^\theta f(\lambda, \mathbf{t})$ extracts the frequency contents of the function $f(\mathbf{t})$ around the frequency coordinates $(\omega_1^0/\lambda, \omega_2^0/\lambda) \equiv (\omega^0 \cos \theta/\lambda, \omega^0 \sin \theta/\lambda)$ with a radial uncertainty of $\sigma_{\hat{\psi}_{\lambda, \mathbf{t}}} = 1/\lambda$, at the location \mathbf{t} . Therefore, by fixing λ and traversing along θ , directional information at a fixed scale λ can be extracted, and by fixing θ and traversing along λ , scale information in a fixed direction can be obtained. Some extensive work has been done in the area of image processing using directionally selective wavelets, such as the two-dimensional Morlet wavelet, in the context of image processing [see *Antoine et al.*, 1992, 1993, and references therein]. This can be potentially applied to the study of geophysical processes. *Kumar* [1995] used a 2-D Morlet wavelet to characterize anisotropy in radar-depicted spatial rainfall by studying the fraction of energy in different directions at different scales. It was found that the methodology revealed even the subtle presence of scale-space anisotropy in random fields. It was concluded that rainfall fields might show anisotropic structure that might not be obvious from a typical spectral analysis and that this information might be important in sampling and modeling.

Often the directional selectivity offered by the Morlet wavelet is not desired, and one wishes to pick frequencies with no preferential direction. *Dallard and Spedding* [1993] defined a wavelet by modifying the Morlet wavelet and called it the halo wavelet because of its shape in the Fourier space. The wavelet itself is defined through its Fourier transform

$$\hat{\psi}(\Omega) = \kappa \exp [-(|\Omega| - |\Omega^0|)^2/2], \quad (44)$$

where κ is a normalizing constant. As can be seen from the above expression, this wavelet has no directional specificity.

Two-dimensional wavelets have found numerous applications in the study of turbulence. The basic idea

behind using wavelet transforms for the study of turbulence is to decouple the dynamics of coherent structures from the residual flow. As is argued by *Fargé et al.* [1996], if one is able to identify the dynamically active structures constituting turbulent flows and classify their elementary interactions, then one can define appropriate conditional averaging procedures by which statistical observables can be constructed. Describing and following the evolution of these observables will then point out what type of nonlinear averaging is needed to go from the Navier-Stokes equations to the fully developed turbulence equations, a problem which still remains open. A detailed discussion of open problems in turbulence addressed using the wavelets as well as a historical survey of applications is given by *Fargé* [1992a] (see also *Fargé* [1992b, c], *Fargé et al.* [1990, 1996], *Everson et al.* [1990], and *Berkooz et al.* [1992]).

Two-dimensional orthogonal wavelets have been developed under the two-dimensional multiresolution framework [*Mallat*, 1989a, b; *Daubechies*, 1988, 1992; *Meyer*, 1992, 1993b]. The mathematical details are beyond the scope of this review, and the reader is referred to the above cited publications for a full account or to *Kumar and Foufoula-Georgiou* [1993a] for a brief description. Here we will concentrate on a few geophysical applications. *Kumar and Foufoula-Georgiou* [1993a, b, c] applied a two-dimensional orthogonal wavelet transform to segregate spatial rainfall into multiscale local averages and multiscale local fluctuations. By analyzing several radar-observed mesoscale convective systems in Oklahoma they concluded that the (so-defined) rainfall fluctuations exhibit scale invariance (simple scaling) and can be modeled through a class of stable distributions. The statistical parameterization of these fluctuations was further studied by *Perica and Foufoula-Georgiou* [1996a], who found that (1) the standardized rainfall fluctuations, that is, the rainfall fluctuations divided by the corresponding-scale average rainfall intensities, exhibited normality and simple scaling between the scales of 4×4 and $64 \times 64 \text{ km}^2$ and (2) the statistical parameterization of these fluctuations was strongly related to a measure of the convective instability of the prestorm environment, namely, the convective available potential energy (CAPE). On the basis of these relationships a multiscale disaggregation model of spatial rainfall was proposed [*Perica and Foufoula-Georgiou*, 1996b]. The model uses an inverse wavelet transform (IWT) to obtain rainfall intensities at any scale smaller than an initial scale (e.g., from 64×64 down to $4 \times 4 \text{ km}^2$ rainfall averages), given the large-scale rainfall average and the value of CAPE (which is used to predict the self-similar parameterizations of rainfall fluctuations). Evaluation of the model in midlatitude mesoscale convective systems showed that it is capable of reconstructing the small-scale statistical variability of rainfall as well as the fraction of area covered by rain. Plate 1 shows one example where the IWT model was used to disaggregate (downscale) rainfall from $64 \times 64 \text{ km}^2$ averages down to $4 \times 4 \text{ km}^2$

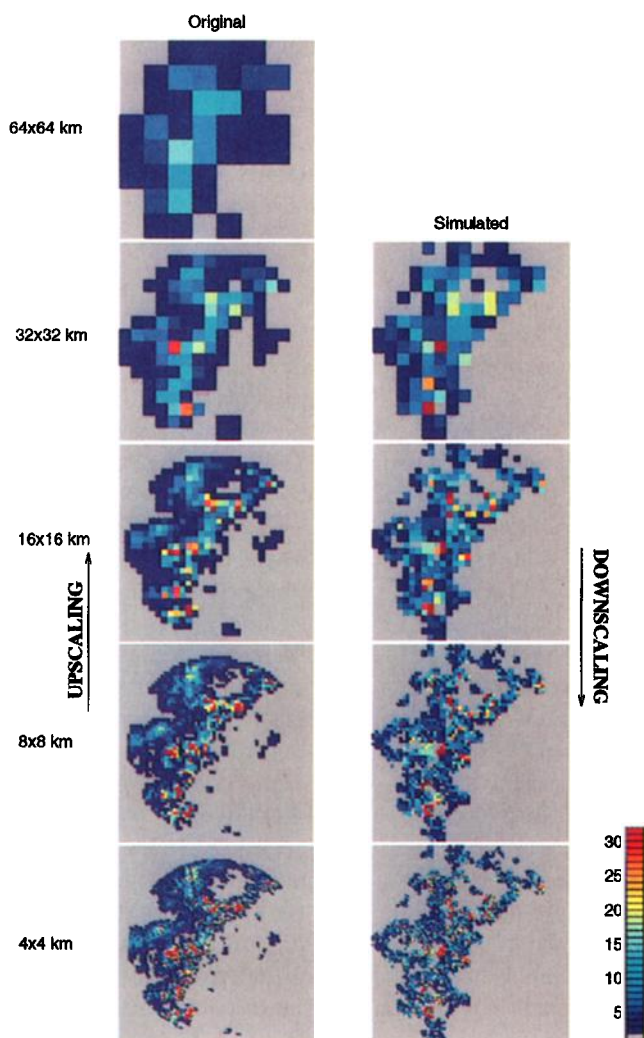


Plate 1. The June 27, 1985, storm over Kansas-Oklahoma at 0300 UTC. The bottom figure in the left column shows the original radar data at $4 \times 4 \text{ km}^2$ resolution. From these data, rainfall fields at lower and lower resolutions (up to $64 \times 64 \text{ km}^2$ averages) were obtained by averaging, and these fields are shown in the left column (upscaling). Then, using the $64 \times 64 \text{ km}^2$ field and the downscaling scheme of *Perica and Foufoula-Georgiou* [1996b], rainfall fields at higher resolutions were reconstructed down to the resolution of $4 \times 4 \text{ km}^2$. A good agreement is seen between the rain patterns and the areas covered by rain of the simulated and original fields at all resolutions. A more rigorous quantitative comparison of several statistical measures of the original and simulated fields is given by *Perica and Foufoula-Georgiou* [1996b]. (Adapted from *Perica and Foufoula-Georgiou* [1996b].)

averages. It is seen that the disaggregated fields at all intermediate scales compare well with actual fields. More details and a formal statistical comparison are given by *Perica and Foufoula-Georgiou* [1996b].

A problem of significant interest in the study of precipitation fields is the segregation of small-scale convective activity from the larger-scale stratiform precipitation. This is of considerable interest in studying the diurnal effect of heating on precipitation, as convective

activity tends to be affected by the diurnal cycle of heating more strongly than the larger-scale stratiform precipitation [*Bell and Suhasini*, 1994]. One of the Tropical Rainfall Measuring Mission (TRMM) objectives is to separate the observed precipitation into its convective and stratiform components, and several methods of achieving this have been proposed [e.g., see *Tokay and Short*, 1996; *Steiner et al.*, 1995]. Some preliminary results using a cosine packet transform, which is a variant of the wavelet packet transform [*Coifman and Meyer*, 1991], show the potential of addressing this problem using a wavelet-based method. Figure 16 shows a 5-min aggregated squall line rainfall observed in Norman, Oklahoma, on May 27, 1987 (see *Kumar and Foufoula-Georgiou* [1993a] for details about the data set). Superimposed on it is a grid which shows the scales of the basis functions found to optimally represent the image. As is clearly seen, small-scale convective activity is identified through layering of small boxes, and the regions bounded by larger boxes correspond to stratiform activity. Research is currently underway to identify the optimal criteria to demarcate the convective and stratiform regions.

7. ON THE CHOICE OF WAVELETS

Different categories of wavelets, such as continuous, discrete, orthogonal, etc., and various types of wavelets

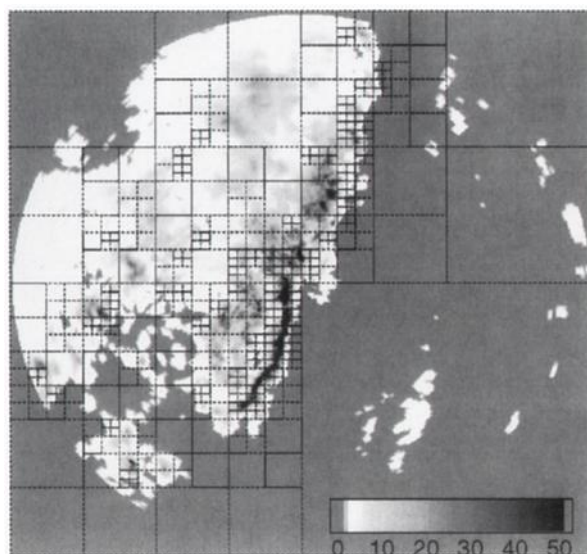


Figure 16. Identification of different scales of activity in a squall line storm. In the background is a 5-min averaged rainfall intensity (in millimeters per hour) of a squall line rainfall observed in Norman, Oklahoma, on May 27, 1987. A radial coverage of 230 km from the radar site is depicted. Superimposed on it is a grid of cells called Heisenberg boxes that shows the scales of the cosine packet basis functions found to optimally characterize the image. The smaller-scale convective activity is identified through layering by small boxes, and the region bounded by larger boxes corresponds to stratiform activity.

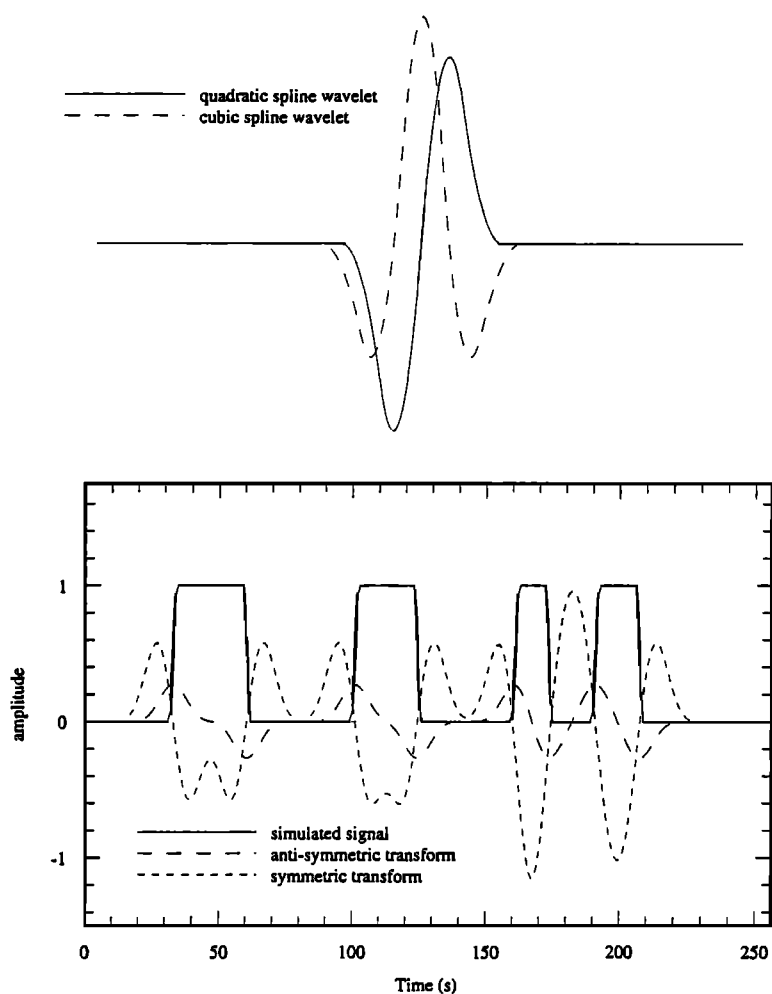


Figure 17. (top) Antisymmetric quadratic spline (solid line) and symmetric cubic spline (dashed lines) wavelets. (bottom) Antisymmetric (long-dashed lines) and symmetric (short-dashed lines) wavelet transforms of a simulated signal (solid line) at the scale 2^3 . (Adapted from *Hagelberg and Gamage* [1994].) (Reprinted by permission of Academic Press.)

within each category provide a multitude of options for us to choose from when analyzing a process of interest. There are several considerations we may use in making our choice, for example, symmetric versus antisymmetric wavelets; continuous wavelets or discrete wavelet frames versus orthogonal wavelets; irregular versus smooth wavelets; physical domain (time or space) versus Fourier domain considerations; and choice of an appropriate wavelet once a given class is chosen.

Hagelberg and Gamage [1994] have illustrated that the magnitude of the wavelet transform using a symmetric wavelet is large at the boundaries of the transition while that using antisymmetric wavelets is large at the center of the transition (see Figure 17). This shows that we can emphasize a region either of sharp transition or of stationary activity by appropriate choice of the wavelet.

The choice between continuous wavelets or discrete wavelet frames and orthogonal wavelets is guided by considerations of the role of redundancy. When we need quantitative information about the process, often orthogonal wavelets provide the best choice. However, in applications such as noise suppression, redundant representation of wavelet frames is an appropriate choice.

Wavelet frames also have attractive sampling properties [*Benedetto*, 1993] and are useful when qualitative or exploratory analysis is required at small increments of scale due to the ability to perform analysis at scales that are finer than dyadic increments.

An irregular or even discontinuous wavelet such as the Haar wavelet often provides a good and simple choice for applications where the process has sharp variations. More sophisticated smoother wavelets sometimes do not provide a better alternative. For example, Figures 9c and 9d illustrate the time-scale analysis of the rainfall time series using the D8 wavelet. In comparison to the Haar wavelet (Figures 9a and 9b) the number of coefficients required to describe the data is comparable (Figures 9b and 9d), showing that at least for these data, smoother wavelets offer no significant advantage due to the irregular nature of the time series.

When strong localization properties in the Fourier domain are desired for applications in filtering, the choice should be guided by considering the spectral properties of the wavelets. For example, although the Haar wavelet is conceptually simple to understand and algorithmically easy to implement, its spectrum is not

well localized, thereby making it inappropriate for filtering applications.

Given a particular class of wavelets, such as *Daubechies*' [1988] orthogonal wavelets, it is often difficult to decide which specific wavelet to use within that class. To address this problem, *Goel and Vidakovic* [1994] observed that our choice should be the wavelet that most "disbalances" the energy of the signal, that is, the wavelet that provides the description of the process in the least number of coefficients (see also Figure 9). They have developed a thresholding scheme called Lorentz thresholding to identify the most significant coefficients and the optimal wavelet for the analysis [see also *Katul and Vidakovic*, 1996].

Clearly, our choice of the analyzing wavelet is determined by a combination of the above considerations, and the appropriate choice should be made and justified on a case by case basis.

8. SUMMARY AND CONCLUSIONS

The purpose of many geophysical studies is to understand the physics and underlying structure of natural processes and to build models that capture some aspects of these processes. Often this is achieved by analyzing observations of the process, extracting important features regarding its morphological and statistical structure, and using this information for model building. On some occasions, physical considerations directly guide model formulation, and in such cases, observations are used to validate or further refine the postulated model.

Most scientists that have been involved with data analysis and model building will attest to the fact that it is as much art as science to model a complex natural process. Certain assumptions have to be always made, and certain aspects of the process variability must often be ignored, depending on the purpose of modeling. Mathematically rigorous tools of analysis that can point to important features of a process and reveal structure not apparent from direct observation are a key component of process understanding. For geophysical processes, in particular, tools that offer the ability to examine the variability of a process at different scales are especially important. The wavelet transform offers such a tool and has already proven useful in the study of many processes in diverse areas of science and engineering.

In this paper we have focused on presenting the most important properties of wavelet transforms that make them attractive for geophysical applications. The key reason for the widespread application of wavelet transforms is the property of time-frequency localization and its ramifications. It is interesting to note that by changing our perspective we can use the same formulation for different applications. On the one hand, wavelet transforms provide a tool for time-frequency localization, and

on the other hand, they provide a tool for time-scale unfolding of the characteristics of the process. We discussed several properties and applications of continuous, discrete, and orthogonal wavelet transforms, the three main classifications of wavelet transforms. We pointed out a major limitation of wavelet transforms, that is, the lack of decoupling between the scale and frequency parameters. Wavelet packets were developed to provide this decoupling, and they thus provide a more refined tool for the study of processes. We discussed this decoupling and some applications of wavelet packets. Along with the mathematical results that are potentially useful for geophysics, our emphasis has been on reviewing the results and insights developed through applications to geophysical processes. We have discussed applications of wavelets in fractal, multifractal, and self-similar stochastic processes, detection of singularities, analysis of nonstationary processes, data compression and filtering, and solution of partial differential equations. Geophysical applications discussed related to turbulence, canopy cover, spatial and temporal rainfall, seafloor bathymetry, ocean wind waves, and remote sensing imaging, among others. It is anticipated that in the near future we will see an explosion of the use of wavelets for the study, analysis, and modeling of geophysical processes. Judiciously used, this higher level of sophistication in our methods of analysis will bring new insights and understanding of many complex phenomena around us.

The detailed discussion of numerical algorithms for implementation of wavelet and wavelet packet transforms was outside the scope of this paper. A basic algorithm for the orthogonal wavelet transform is discussed in the appendix. Here we only give the reader some key references. A fast algorithm for implementation of the orthogonal wavelet transform was developed by *Mallat* [1989a, b] (see also a brief summary of the algorithm in Appendix C of *Kumar and Foufoula-Georgiou* [1994]). An implementation algorithm for the discrete nonorthogonal wavelet transform is given by *Shensa* [1993]. Algorithms and programs for wavelet and wavelet packet applications are given by *Wickerhauser* [1994] [see also *Press et al.*, 1992]. Also, a wavelet transform module is available through a commercial package called Splus (available from StatSci Division of MathSoft, Inc., Seattle, Washington) for exploratory and advanced data analysis. The wavelet transform has also been recently incorporated into signal processing packages such as MATLAB (an older version is available by anonymous ftp from simplicity.stanford.edu). Other wavelet-related software is often available from anonymous ftp sites (e.g., see *Kumar and Foufoula-Georgiou* [1994] for a list). The reader is encouraged to experiment with these packages for hands-on understanding of the wavelet analysis capabilities and their usefulness in studying geophysical processes.

APPENDIX: COMPUTATIONAL ASPECTS OF ORTHOGONAL WAVELET TRANSFORMS

The algorithm for implementation of the multiresolution wavelet transform is simple. From a data sequence $\{c_n^0\}$ (say, at resolution level $m = 0$) corresponding to a function $f(t)$ we construct

$$P_0 f(t) = \sum_n c_n^0 \phi(t - n) \quad (45)$$

for a chosen $\phi(t)$, that is, assume $\{c_n^0\}_{n \in \mathbf{Z}} = \{(f, \phi_{0n})\}_{n \in \mathbf{Z}}$. The data sequence at lower resolution can be obtained using a discrete filter $\{h(n)\}$ (obtained from $\phi_{0n}(t)$) as

$$c_k^{-1} = \sum_n h(n - 2k) c_n^0. \quad (46)$$

The detail sequence $\{d_k^{-1}\}_{k \in \mathbf{Z}} = \{(f, \psi_{-1k})\}_{k \in \mathbf{Z}}$ is obtained as

$$d_k^{-1} = \sum_n g(n - 2k) c_n^0, \quad (47)$$

where $\{g(n)\}$ is a discrete filter. See Daubechies [1992] for the values of $h(n)$ and $g(n)$ for different choices of $\phi(t)$ and $\psi(t)$. Equivalently, equations (46) and (47) can be written in the matrix notation:

$$\{c^{-1}\} = H\{c^0\} \quad \{d^{-1}\} = G\{c^0\}. \quad (48)$$

The matrices H and G are such that

$$HH^* = I \quad GG^* = I \quad (49)$$

and H^*H and G^*G are mutually orthogonal projections with

$$H^*H + G^*G = I, \quad (50)$$

where H^* and G^* are adjoints of H and G , respectively, and I is the identity matrix. Also,

$$GH^* = 0 \quad HG^* = 0. \quad (51)$$

The algorithm given in (46) and (47) can be recursively implemented, and the data and detail sequence at lower and lower resolutions can be obtained. The inverse transformation, from the lower to higher resolution, can be obtained using

$$c_n^m = 2 \sum_k h(n - 2k) c_k^{m-1} + 2 \sum_k g(n - 2k) d_k^{m-1} \quad (52)$$

and it gives an exact reconstruction.

ACKNOWLEDGMENTS. The first author acknowledges the support of the University of Illinois Research Board and NASA grants NASA-NAGW-5247 and NASA-NAG5-3661. The second author acknowledges the support of National Science Foundation grant EAR-9117866, NASA grant NAG 5-2108, and NOAA grant NA46GP0486. Along the course of our research on wavelet transforms, computing resources were kindly provided by the Minnesota Supercomputer Institute.

We also thank Venugopal Vuruputur for many useful comments on an earlier draft of this manuscript and Marc Parlange and Gabriel Katul for providing us with the surface flux measurements in Owens Valley.

James A. Smith was the editor responsible for this paper. He and the authors thank Gabriel Katul and an anonymous reviewer for their technical reviews.

REFERENCES

- Allan, D. W., Statistics of atomic frequency clocks, *Proc. IEEE*, *31*, 221–230, 1966.
- Antoine, J., P. Carrette, and R. Murenzi, The scale-angle representation in image analysis with 2D wavelet transform, in *Signal Processing VI: Theories and Applications*, edited by J. Vandewalle et al., pp. 701–704, North-Holland, New York, 1992.
- Antoine, J., P. Carrette, R. Murenzi, and B. Piette, Image analysis with two dimensional continuous wavelet transform, *Signal Process.*, *31*, 241–272, 1993.
- Arnéodo, A., G. Grasseau, and M. Holschneider, Wavelet transform of multifractals, *Phys. Rev. Lett.*, *61*, 2281–2284, 1988.
- Bell, T. L., and R. Suhasini, Principal modes of variation of rain-rate probability distributions, *J. Appl. Meteorol.*, *33*, 1067–1078, 1994.
- Benedetto, J. J., Frame decompositions, sampling, and uncertainty principle inequalities, in *Wavelets: Mathematics and Applications*, edited by J. J. Benedetto, and M. W. Frazier, pp. 247–304, CRC Press, Boca Raton, Fla., 1993.
- Benedetto, J. J., and M. W. Frazier (Eds.), *Wavelets: Mathematics and Applications*, 575 pp., CRC Press, Boca Raton, Fla., 1993.
- Benzi, R., and M. Vergassola, Optimal wavelet analysis and its application to two-dimensional turbulence, *Fluid Dyn. Res.*, *8*, 117–126, 1991.
- Benzi, R., L. Biferale, A. Crisanti, G. Paladin, M. Vergassola, and A. Vulpiani, A random process for the construction of multiaffine fields, *Physica D*, *65*, 352–358, 1993.
- Berkooz, G., J. Elezgaray, and P. Holmes, Coherent structures in random media and wavelets, *Physica D*, *61*, 47–58, 1992.
- Beylkin, G., R. R. Coifman, I. Daubechies, S. G. Mallat, Y. Meyer, L. A. Raphael, and M. B. Ruskai (Eds.), *Wavelets and Their Applications*, Jones and Bartlett, Boston, Mass., 1991.
- Bloschl, G., and M. Sivapalan, Scale issues in hydrological modelling: A review, in *Scale Issues in Hydrological Modelling*, edited by J. D. Kalma and M. Sivapalan, pp. 9–48, John Wiley, New York, 1995.
- Brunet, Y., and S. Collineau, Wavelet analysis of diurnal and nocturnal turbulence above a maize crop, in *Wavelets in Geophysics*, edited by E. Foufoula-Georgiou and P. Kumar, pp. 129–150, Academic, San Diego, Calif., 1994.
- Chui, C. K., *Wavelet Analysis and Its Applications*, vol. 1, *An Introduction to Wavelets*, Academic, San Diego, Calif., 1992a.
- Chui, C. K., *Wavelet Analysis and Its Applications*, vol. 2, *Wavelets—A Tutorial in Theory and Applications*, Academic, San Diego, Calif., 1992b.
- Claasen, T. A. C. M., and W. F. G. Mecklenbrauker, The Wigner distribution—A tool for time-frequency signal analysis, *Philips J. Res.*, *35*, 217–250, 1980.
- Coifman, R., and Y. Meyer, Remarques sur l'analyse de Fourier à fenêtre, *C. R. Acad. Sci., Paris*, *312*, 259–261, 1991.
- Coifman, R. R., Y. Meyer, and V. Wickerhauser, Wavelet analysis and signal processing, in *Wavelets and Their Appli-*

- cations, edited by M. B. Ruskai et al., pp. 153–178, Jones and Bartlett, Boston, Mass., 1992a.
- Coifman, R. R., Y. Meyer, and V. Wickerhauser, Size properties of wavelet-packets, in *Wavelets and Their Applications*, edited by M. B. Ruskai, pp. 453–470, Jones and Bartlett, Boston, Mass., 1992b.
- Collineau, S., and Y. Brunet, Detection of turbulent coherent motions in a forest canopy, I, Wavelet analysis, *Boundary Layer Meteorol.*, *65*, 357–379, 1993a.
- Collineau, S., and Y. Brunet, Detection of turbulent coherent motions in a forest canopy, II, Time-scales and conditional averages, *Boundary Layer Meteorol.*, *66*, 49–73, 1993b.
- Dallard, T., and G. R. Spedding, 2-D wavelet transforms: Generalization on the Hardy space and application to experimental studies, *Eur. J. Mech. Fluids*, *12*(1), 107–134, 1993.
- Daubechies, I., Orthonormal bases of compactly supported wavelets, *Commun. Pure Appl. Math.*, *XLI*, 901–996, 1988.
- Daubechies, I., The wavelet transform, time-frequency localization and signal analysis, *IEEE Trans. Inf. Theory*, *36*(5), 961–1005, 1990.
- Daubechies, I., *Ten Lectures on Wavelets*, 357 pp., Soc. for Ind. and Appl. Math., Philadelphia, Pa., 1992.
- Daubechies, I., Review of *Wavelets and Operators* by Y. Meyer (Cambridge Univ. Press, New York, 1993) and *Wavelets: Algorithms and Applications* by Y. Meyer, (Soc. for Ind. and Appl. Math., Philadelphia, 1993) *Science*, *262*, 1589–1591, 1993.
- Daubechies, I., and J. C. Lagarias, Two-scale difference equations, I, Existence and global regularity of solutions, *SIAM J. Math. Anal.*, *22*(5), 1388–1410, 1991.
- Daubechies, I., and J. C. Lagarias, Two-scale difference equations, II, Local regularity, infinite products of matrices and fractals, *SIAM J. Math. Anal.*, *23*(4), 1031–1079, 1992.
- Daubechies, I., S. Mallat, and A. S. Willsky, Introduction to the special issue on wavelet transforms and multiresolution signal analysis, *IEEE Trans. Inf. Theory*, *38*(2), 529–531, 1992.
- Davis, G., Adaptive nonlinear approximations, Ph.D. thesis, Dep. of Math., Courant Inst. of Math. Sci., New York Univ., New York, 1994.
- Donoho, D. L., and I. M. Johnstone, Ideal spatial adaptation via wavelet shrinkage, *Biometrika*, *81*, 425–455, 1994.
- Everson, R., L. Sirovich, and K. R. Sreenivasan, Wavelet analysis of the turbulent jet, *Phys. Lett. A*, *146*, 314–322, 1990.
- Fargé, M., Wavelet transforms and their applications to turbulence, *Annu. Rev. Fluid Mech.*, *24*, 395–457, 1992a.
- Fargé, M., The continuous wavelet transform of two-dimensional turbulent flows, in *Wavelets and Their Applications*, edited by M. B. Ruskai et al., pp. 275–302, Jones and Bartlett, Boston, Mass., 1992b.
- Fargé, M., The continuous wavelet transform of two-dimensional turbulent flows, in *Wavelets and Their Applications*, edited by M. Ruskai et al., pp. 275–302, Jones and Bartlett, Boston, Mass., 1992c.
- Fargé, M., M. Holschneider, and J. F. Colonna, Wavelet analysis of coherent structures in two-dimensional turbulent flows, in *Topological Fluid Mechanics*, edited by H. K. Moffatt, pp. 765–776, Cambridge Univ. Press, New York, 1990.
- Fargé, M., E. Goirand, Y. Meyer, F. Pascal, and M. V. Wickerhauser, Improved predictability of two-dimensional turbulent flows using wavelet packet compression, *Fluid Dyn. Res.*, *10*(4–6), 229–250, 1992.
- Fargé, M., J. R. Hunt, and J. C. Vassilicos (Eds.), *Wavelets, Fractals and Fourier Transforms: New Developments and New Applications*, Oxford Univ. Press, New York, 1993.
- Fargé, M., N. Kevlahan, V. Perrier, and E. Goirand, Wavelets and turbulence, *Proc. IEEE*, *84*, 639–669, 1996.
- Flandrin, P., Time-frequency and time-scale, in *Proceedings of the 4th Acoustic, Speech and Signal Processing Workshop on Spectrum Estimation Modeling*, pp. 77–80, Inst. of Electr. and Electron. Eng., New York, 1988.
- Flandrin, P., Wavelet analysis and synthesis of fractional Brownian motion, *IEEE Trans. Inf. Theory*, *38*(2), 910–916, 1992.
- Foufoula-Georgiou, E., and P. Kumar, *Wavelets in Geophysics*, 384 pp., Academic, San Diego, Calif., 1994.
- Gamage, N. K. K., and W. Blumen, Comparative analysis of low level cold fronts: Wavelet, Fourier, and empirical orthogonal function decompositions, *Mon. Weather Rev.*, *121*, 2867–2878, 1993.
- Gamage, N. K. K., and C. Hagelberg, Detection and analysis of microfronts and associated coherent events using localized transforms, *J. Atmos. Sci.*, *50*(5), 750–756, 1993.
- Gambis, D., Wavelet transform analysis of the length of the day and the El-Niño/Southern Oscillation variations at intraseasonal and interannual time scales, *Ann. Geophys.*, *10*, 331–371, 1992.
- Gao, W., and B. L. Li, Wavelet analysis of coherent structures at the atmosphere-forest interface, *J. Appl. Meteorol.*, *32*, 1717–1725, 1993.
- Georgakakos, K. P., A. A. Carsteanu, P. L. Sturdevant, and J. A. Cramer, Observation and analysis of midwestern rain-rates, *J. Appl. Meteorol.*, *33*, 1433–1444, 1994.
- Glowinski, R., W. M. Lawton, M. Ravachol, and E. Tenenbaum, Wavelet solutions of linear and nonlinear elliptic, parabolic and hyperbolic problems in one space dimension, in *Computing Methods in Applied Sciences and Engineering*, edited by R. Glowinski and A. Liehnewsky, pp. 55–120, Soc. of Ind. and Appl. Math., Philadelphia, Pa., 1990.
- Goel, P., and B. Vidakovic, Wavelet transformations as diversity enhancers, *Discuss. Pap. 95-08*, Inst. of Stat. and Decis. Sci., Duke Univ., Durham, N. C., 1994.
- Goupillaud, P., A. Grossmann, and J. Morlet, Cycle-octaves and related transforms in seismic signal analysis, *Geoprospection*, *23*, 85–102, 1984.
- Grossmann, A., and J. Morlet, Decomposition of Hardy functions into square integrable wavelets of constant shape, *SIAM J. Math. Anal.*, *15*(4), 723–736, 1984.
- Grossmann, A., R. Kronland-Martinet, and J. Morlet, Reading and understanding continuous wavelet transforms, in *Wavelets: Time-Frequency Methods and Phase Space*, edited by J. Combes, A. Grossmann, and P. Tchamitchian, pp. 2–20, Springer-Verlag, New York, 1989.
- Hagelberg, C., and N. K. K. Gamage, Application of structure preserving wavelet decomposition to intermittent turbulence: A case study, in *Wavelets in Geophysics*, edited by E. Foufoula-Georgiou and P. Kumar, pp. 45–80, Academic, San Diego, Calif., 1994.
- Holschneider, M., Localization properties of wavelet transforms, *J. Math. Phys.*, *34*(7), 3227–3244, 1993.
- Holschneider, M., *Wavelets: An Analysis Tool*, 423 pp., Oxford Sci., New York, 1995.
- Howell, J. F., and L. Mahrt, An adaptive decomposition: Application to turbulence, in *Wavelets in Geophysics*, edited by E. Foufoula-Georgiou and P. Kumar, pp. 107–128, Academic, San Diego, Calif., 1994.
- Hubbard, B. B., *The World According to Wavelets*, 264 pp., A. K. Peters, Wellesley, Mass., 1996.
- Hudgins, L. H., C. A. Friehe, and M. E. Mayer, Fourier and wavelet analysis of atmospheric turbulence, in *Progress in Wavelet Analysis and Applications*, edited by Y. Meyer and S. Roques, pp. 491–498, Frontiers, Gif-sur-Yvette, France, 1993a.
- Hudgins, L. H., C. A. Friehe, and M. E. Mayer, Wavelet transform and atmospheric turbulence, *Phys. Rev. Lett.*, *71*, 3279–3282, 1993b.

- Katul, G. G., and B. Vidakovic, The partitioning of attached and detached eddy motion in the atmospheric surface layer using Lorentz wavelet filtering, *Boundary Layer Meteorol.*, 77, 153–172, 1996.
- Katul, G. G., J. D. Albertson, C. R. Chu, and M. B. Parlange, Intermittency in atmospheric turbulence using orthonormal wavelets, in *Wavelets in Geophysics*, edited by E. Foufoula-Georgiou and P. Kumar, pp. 81–105, Academic, San Diego, Calif., 1994.
- Kumar, P., A wavelet-based methodology for scale-space anisotropic analysis, *Geophys. Res. Lett.*, 22(20), 2777–2780, 1995.
- Kumar, P., Role of coherent structures in the stochastic-dynamic variability of precipitation, *J. Geophys. Res.*, 101(D21), 26,393–26,404, 1996.
- Kumar, P., and E. Foufoula-Georgiou, A multicomponent decomposition of spatial rainfall fields, 1, Segregation of large- and small-scale features using wavelet transforms, *Water Resour. Res.*, 29(8), 2515–2532, 1993a.
- Kumar, P., and E. Foufoula-Georgiou, A multicomponent decomposition of spatial rainfall fields, 2, Self-similarity in fluctuations, *Water Resour. Res.*, 29(8), 2533–2544, 1993b.
- Kumar, P., and E. Foufoula-Georgiou, A new look at rainfall fluctuations and scaling properties of spatial rainfall using orthogonal wavelets, *J. Appl. Meteorol.*, 32, 209–222, 1993c.
- Kumar, P., and E. Foufoula-Georgiou, Wavelet analysis in geophysics: An introduction, in *Wavelets in Geophysics*, edited by E. Foufoula-Georgiou and P. Kumar, pp. 1–43, Academic, San Diego, Calif., 1994.
- Liu, P., Wavelet spectrum analysis and ocean wind waves, in *Wavelets in Geophysics*, edited by E. Foufoula-Georgiou and P. Kumar, pp. 151–166, Academic, San Diego, Calif., 1994.
- Mallat, S., A theory for multiresolution signal decomposition: The wavelet representation, *IEEE Trans. Pattern Anal. Mach. Intel.*, 11(7), 674–693, 1989a.
- Mallat, S., Multifrequency channel decomposition of images and wavelet models, *IEEE Trans. Acoust. Speech Signal Anal.*, 37(12), 2091–2110, 1989b.
- Mallat, S. G., and Z. Zhang, Matching pursuits with time-frequency dictionaries, *IEEE Trans. Signal Process.*, 41(12), 3397–3415, 1993.
- Mandelbrot, B., and J. Van Ness, Fractional Brownian motions, fractional noises and applications, *SIAM Rev.*, 10(4), 422–437, 1968.
- Marr, D., *Vision*, 397 pp., W. H. Freeman, New York, 1982.
- Meneveau, C., Analysis of turbulence in the orthonormal wavelet representation, *J. Fluid Mech.*, 232, 469–520, 1991a.
- Meneveau, C., Dual spectra and mixed energy cascade of turbulence in the wavelet representation, *Phys. Rev. Lett.*, 11, 1450–1453, 1991b.
- Meyer, Y., *Wavelets and Operators*, Cambridge Univ. Press, New York, 1992.
- Meyer, Y., Review of *An Introduction to Wavelets* by C. K. Chui and *Ten Lectures on Wavelets* by I. Daubechies, *Bull. Am. Math. Soc.*, 28(2), 350–360, 1993a.
- Meyer, Y., *Wavelets: Algorithms and Applications*, Soc. of Ind. and Appl. Math., Philadelphia, Pa., 1993b.
- Meyer, Y., and S. Roques, *Progress in Wavelet Analysis and Applications*, Frontières, Gif-sur-Yvette, France, 1993.
- Morlet, J., G. Arens, E. Fourgeau, and D. Giard, Wave propagation and sampling theory, 1, Complex signal and scattering in multilayered media, *Geophysics*, 47(2), 203–221, 1982a.
- Morlet, J., G. Arens, E. Fourgeau, and D. Giard, Wave propagation and sampling theory, 2, Sampling theory and complex waves, *Geophysics*, 47(2), 222–236, 1982b.
- Papoulis, A., *The Fourier Integral and Its Applications*, 318 pp., McGraw-Hill, New York, 1962.
- Percival, D. B., and P. Guttorp, Long-memory processes, the Allan variance and wavelets, in *Wavelets in Geophysics*, edited by E. Foufoula-Georgiou and P. Kumar, pp. 325–344, Academic, San Diego, Calif., 1994.
- Perica, S., and E. Foufoula-Georgiou, Linkage of scaling and thermodynamic parameters of rainfall: Results from mid-latitude mesoscale convective systems, *J. Geophys. Res.*, 101(D3), 7431–7448, 1996a.
- Perica, S., and E. Foufoula-Georgiou, Model for multiscale disaggregation of spatial rainfall based on coupling meteorological and scaling descriptions, *J. Geophys. Res.*, 101(D21), 26,347–26,361, 1996b.
- Perrier, V., Towards a method for solving partial differential equations using wavelet bases, in *Wavelets: Time-Frequency Methods and Phase-Space*, edited by J. M. Combes et al., pp. 269–283, Springer-Verlag, New York, 1990.
- Press, W. H., S. A. Teukolsky, W. T. Vetterling, and B. P. Flannery, *Numerical Recipes*, 994 pp., Cambridge Univ. Press, New York, 1992.
- Qian, S., and J. Weiss, Wavelets and the numerical solution of partial differential equations, *J. Comput. Phys.*, 106, 155–175, 1993.
- Ramanathan, J., and O. Zeitouni, On the wavelet transform of fractional Brownian motion, *IEEE Trans. Inf. Theory*, 37(4), 1156–1158, 1991.
- Rioul, O., A discrete time multiresolution theory, *IEEE Trans. Signal Process.*, 41(10), 2591–2606, 1993.
- Rioul, O., and M. Vetterli, Wavelets and signal processing, *IEEE Signal Process. Mag.*, 8(4), 14–38, 1991.
- Robinson, S. K., Coherent motion in turbulent boundary layer, *Annu. Rev. Fluid Mech.*, 23, 601–639, 1991.
- Ruskai, M. B., G. Beylkin, R. Coifman, I. Daubechies, S. Mallat, Y. Meyers, and L. Raphael (Eds.), *Wavelets and Their Applications*, Jones and Bartlett, Boston, Mass., 1992.
- Saito, N., Simultaneous noise suppression and signal compression using a library of orthonormal bases and the minimum description length criteria, in *Wavelets in Geophysics*, edited by E. Foufoula-Georgiou and P. Kumar, pp. 299–324, Academic, San Diego, Calif., 1994.
- Schultz, R. L., and H. W. Wyld, Using wavelets to solve the Burgers equation—A comparative study, *Phys. Rev. A*, 46(12), 7953–7958, 1992.
- Sellers, P. J., F. G. Hall, G. Asrar, D. E. Strelbel, and R. E. Murphy, An overview of the First International Satellite Land Surface Climatology Project (ISLSCP) Field Experiment (FIFE), *J. Geophys. Res.*, 97(D17), 18,345–18,371, 1992.
- Shensa, M. J., An inverse DWT for nonorthogonal wavelets, *Tech. Rep. TR 1621*, Nav. Command and Ocean Surveillance Cent., San Diego, Calif., July 1993.
- Steiner, M., R. A. Houze Jr., and S. E. Yuter, Climatological characterization of three-dimensional storm structure from operational and raingage data, *J. Appl. Meteorol.*, 34, 1978–2007, 1995.
- Teti, J. G., and H. N. Kritikos, SAR ocean image representation using wavelets, *IEEE Trans. Geosci. Remote Sens.*, 30(5), 1089–1094, 1992.
- Tewfik, A. H., and M. Kim, Correlation structure of the discrete wavelet coefficients of fractional Brownian motion, *IEEE Trans. Inf. Theory*, 38(2), 904–909, 1992.
- Tokay, A., and D. Short, Evidence from tropical raindrop spectra of the origin of rain from stratiform versus convective clouds, *J. Appl. Meteorol.*, 35, 355–371, 1996.
- Tukey, J. W., *Exploratory Data Analysis*, 688 pp., Addison-Wesley, Reading, Mass., 1977.
- Turner, B. J., M. Y. Leclerc, M. Gauthier, K. E. Moore, and D. R. Fitzjarrald, Identification of turbulence structures above a forest canopy using a wavelet transform, *J. Geophys. Res.*, 99(D1), 1919–1926, 1994.

- Venugopal, V., and E. Fofoula-Georgiou, Time-frequency-scale analysis of high resolution temporal rainfall using wavelet packets, *J. Hydrol.*, 187, 3–27, 1996.
- Vetterli, M., and C. Herley, Wavelets and filter banks: Theory and design, *IEEE Trans. Signal Process.*, 40(9), 2207–2232, 1992.
- Wickerhauser, M. V., Acoustic signal compression with wavelet packets, in *Wavelets—A Tutorial in Theory and Applications*, edited by C. K. Chui, pp. 679–700, Academic, San Diego, Calif., 1992.
- Wickerhauser, M. V., *Adapted Wavelet Analysis From Theory to Software*, 486 pp., A. K. Peters, Wellesley, Mass., 1994.
- Wornell, G. W., A Karhunen-Loève-like expansion for $1/f$ -processes via wavelets, *IEEE Trans. Inf. Theory*, 36(4), 859–861, 1990.
- Wornell, G. W., *Signal Processing With Fractals: A Wavelet-Based Approach*, Prentice-Hall, Englewood Cliffs, N. J., 1995.
- Xu, J.-C., and W.-C. Shann, Galerkin-wavelet methods for two-point boundary-value-problems, *Numer. Math.*, 63(1), 123–144, 1992.
- Yamada, M., and K. Ohkitani, Orthonormal wavelet expansion and its application to turbulence, *Prog. Theor. Phys.*, 83(5), 819–823, 1990.
- Yamada, M., and K. Ohkitani, Orthonormal wavelet analysis of turbulence, *Fluid Dyn. Res.*, 8, 101–115, 1991a.
- Yamada, M., and K. Ohkitani, An identification of energy cascade in turbulence by orthonormal wavelet analysis, *Prog. Theor. Phys.*, 86(4), 799–815, 1991b.

E. Fofoula-Georgiou, St. Anthony Falls Laboratory, Department of Civil Engineering, University of Minnesota, Minneapolis, MN 55414. (e-mail: efi@mykonos.safhl.umn.edu)

P. Kumar, Hydrosystems Laboratory, Department of Civil Engineering, University of Illinois, Urbana, IL 61801. (e-mail: kumar1@uiuc.edu)